Title

Influence of Hydrological Perturbations and Riverbed Sediment Characteristics on Hyporheic Zone Respiration of CO2 and N2

Journal

Journal of Geophysical Research Biogeosciences, 123(3)

ISSN

2169-8953

Authors

Newcomer, Michelle E
Hubbard, Susan S
Fleckenstein, Jan H
et al.

Publication Date

2018-03-01

DOI

10.1002/2017jg004090

Peer reviewed

AGU PUBLICATIONS

JGR

Journal of Geophysical Research: Biogeosciences

RESEARCH ARTICLE

10.1002/2017JG004090

Key Points:
- Hyporheic zone sediments and water tables control hyporheic respiration and denitrification
- Losing rivers store C and N that enter the system as biomass and dissolved gases
- Gaining rivers release majority of microbial end products as gases

Supporting Information:
- Supporting Information S1
- Data Set S1

Correspondence to:
Y. Rubin,
rubin@ce.berkeley.edu

Citation:
Newcomer, M. E., Hubbard, S. S., Fleckenstein, J. H., Maier, U., Schmidt, C., Thullner, M., et al. (2018). Influence of hydrological perturbations and riverbed sediment characteristics on hyporheic zone respiration of CO_2 and N_2. *Journal of Geophysical Research: Biogeosciences*, *123*. https://doi.org/10.1002/2017JG004090

Received 31 JUL 2017
Accepted 14 FEB 2018
Accepted article online 22 FEB 2018

Influence of Hydrological Perturbations and Riverbed Sediment Characteristics on Hyporheic Zone Respiration of CO_2 and N_2

Michelle E. Newcomer[1], Susan S. Hubbard[1], Jan H. Fleckenstein[2], Ulrich Maier[3], Christian Schmidt[2], Martin Thullner[4], Craig Ulrich[1], Nicolas Flipo[5], and Yoram Rubin[6]

[1]Climate and Ecosystem Sciences Division, Lawrence Berkeley National Laboratory, Berkeley, CA, USA, [2]Department of Hydrogeology, Helmholtz-Centre for Environmental Research, UFZ, Leipzig, Germany, [3]Department of Applied Geology, Geoscience Centre of the University of Göttingen, Göttingen, Germany, [4]Department of Environmental Microbiology, Helmholtz-Centre for Environmental Research, UFZ, Leipzig, Germany, [5]Geosciences Department, MINES ParisTech, PSL Research University, Paris, France, [6]Department of Civil and Environmental Engineering, University of California, Berkeley, CA, USA

Abstract Rivers in climatic zones characterized by dry and wet seasons often experience periodic transitions between losing and gaining conditions across the river-aquifer continuum. Infiltration shifts can stimulate hyporheic microbial biomass growth and cycling of riverine carbon and nitrogen leading to major exports of biogenic CO_2 and N_2 to rivers. In this study, we develop and test a numerical model that simulates biological-physical feedback in the hyporheic zone. We used the model to explore different initial conditions in terms of dissolved organic carbon availability, sediment characteristics, and stochastic variability in aerobic and anaerobic conditions from water table fluctuations. Our results show that while highly losing rivers have greater hyporheic CO_2 and N_2 production, gaining rivers allowed the greatest fraction of CO_2 and N_2 production to return to the river. Hyporheic aerobic respiration and denitrification contributed 0.1–2 g/m^2/d of CO_2 and 0.01–0.2 g/m^2/d of N_2; however, the suite of potential microbial behaviors varied greatly among sediment characteristics. We found that losing rivers that consistently lacked an exit pathway can store up to 100% of the entering C/N as subsurface biomass and dissolved gas. Our results demonstrate the importance of subsurface feedbacks whereby microbes and hydrology jointly control fate of C and N and are strongly linked to wet-season control of initial sediment conditions and hydrologic control of seepage direction. These results provide a new understanding of hydrobiological and sediment-based controls on hyporheic zone respiration, including a new explanation for the occurrence of anoxic microzones and large denitrification rates in gravelly riverbeds.

Plain Language Summary River systems are important components of our landscape that help to degrade contaminants, support food webs, and transform organic matter. In this study, we developed and tested a model that could help reveal the role of the riverbed for these ecosystem services. We used the model to explore how different riverbed conditions eventually control the fate of carbon and nitrogen. Our results show that carbon and nitrogen transformations and the potential suite of microbial behaviors are dependent on the riverbed sediment structure and the water table conditions in the local groundwater system. The implications of this are that the riverbed sediments and the cumulative effect of water table conditions can control hyporheic processing. Under future river discharge conditions, assuming reduced river flows and siltation of riverbeds, reductions in total hyporheic processing may be observed.

1. Introduction

Despite their small areal extent, rivers are increasingly recognized as significant hot spots for global carbon (C) and nitrogen (N) degradation and associated greenhouse gas emissions (Battin et al., 2016; Gomez-Velez et al., 2015; Höpfner et al., 2012; Hotchkiss et al., 2015; Peyrard et al., 2011). The significance of biogenic CO_2 and N_2 gas production due to heterotrophic microbial activity in rivers and associated hyporheic zones to the overall carbon balance of rivers is poorly quantified, yet net heterotrophy is estimated to be 0.32 Pg C yr^{-1}, with half of terrestrial organic carbon stored or transformed in aquatic systems (Battin et al., 2008). While net heterotrophic conditions are common in inland waters (Escoffier et al., 2016), much less is known about controls on hyporheic zone contributions to biogenic CO_2 and N_2 gas production and fate of resulting C and N storage in subsurface biomass.

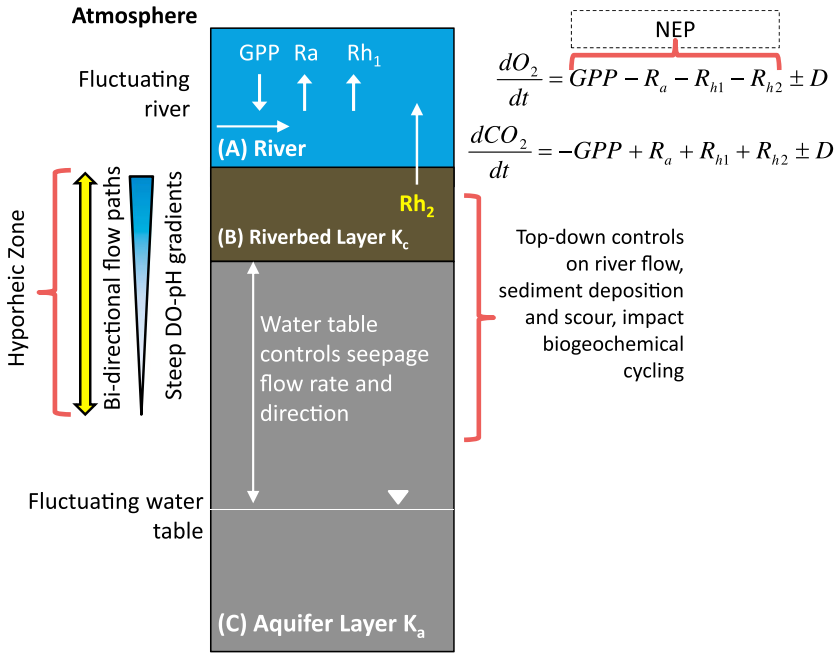

Figure 1. Geometry of the 1-D river, aquifer, and hyporheic zone compartment conceptual model setup. The exchange of nutrients, water fluxes, and gases across the hyporheic zone occurs because of bidirectional flow paths and steep DO-pH gradients. Head boundary conditions are implemented on the top and bottom of the model to represent the river and the groundwater table. Riverbed and aquifer hydraulic conductivities are shown as K_c and K_a, respectively. NEP = net ecosystem production; GPP = gross primary production; R_a = autotrophic respiration; $R_{h1} + R_{h2}$ = river and hyporheic heterotrophic respiration; D = diffusion.

As a zone that links the river and aquifer compartments, hyporheic zones represent a transitional region important for a multitude of ecosystem services (J. W. Harvey & Gooseff, 2015; Larned et al., 2015). Hyporheic zones support heterotrophic microbial aerobic respiration (AR), anaerobic denitrification (DN), and nitrification (NI) (Gomez-Velez et al., 2015; J. W. Harvey et al., 2013), processes that transform a significant percentage of terrestrial organic matter (Casas-Ruiz et al., 2016; Findlay, 1995; Rode et al., 2015). Here we define the hyporheic zone as the portion of the sediment where biogeochemical conditions are influenced by the bidirectional supply of nutrients from the stream or aquifer across steep redox gradients (Figure 1). In addition to redox reactions, hyporheic zones can store river C and N in interstitial microbial biomass in riverbed sediments across sharp oxic-anoxic fronts (Caruso et al., 2017). Despite the importance of rivers and hyporheic zones for these ecosystem services, the role of the hyporheic zone and controls on the rates of these processes still remains poorly understood across landscapes, climates, and scales within a watershed (J. W. Harvey & Gooseff, 2015; Ranalli & Macalady, 2010).

Hyporheic zones contribute to metrics of river net ecosystem productivity (NEP) through the consumption of O_2 from AR and NI and the production of CO_2 from both AR and DN. NEP is typically estimated with instream diel oxygen metabolism methods (i.e., Escoffier et al., 2016; Hall et al., 2015; Hotchkiss et al., 2015; Odum, 1956), as a balance between gross primary production (GPP), autotrophic respiration (R_a), and river and hyporheic heterotrophic respiration ($R_{h1} + R_{h2}$) where the hyporheic heterotrophic component (R_{h2}) is typically neglected in the O_2 model (Figure 1). Assuming a 1:1 ratio between O_2 consumption and CO_2 production ($\frac{dO_2}{dt} = -\frac{dCO_2}{dt}$), and constant diffusion terms (D), hyporheic heterotrophic respiration (R_{h2}) is then estimated using river CO_2 mass balance closure with rates of R_{h2} found to vary between 1 and 2 g/m^2/d of CO_2 (Hotchkiss et al., 2015). DN rates have been estimated from hyporheic studies ranging between 0.1 and 0.4 g/m^2/d of N_2 (J. W. Harvey et al., 2013).

Our fundamental understanding of the controls on AR and DN within hyporheic zones is linked to the accurate representation of the physical conditions of this zone (Figure 1). Physical characteristics can vary dynamically with time as a function of microbial growth and infiltration within riverbed sediments representing

an internal control on AR and DN (Newcomer et al., 2016). As microbial populations increase (Rosenzweig et al., 2014; Thullner, 2010; Yarwood et al., 2006), biofilms and cellular matter associated with their growth fill sediment pore spaces, reducing riverbed porosity (Φ) and riverbed hydraulic conductivity (K_c) (Brovelli et al., 2009; Thullner, Mauclaire, et al., 2002; Thullner et al., 2004; Thullner, Zeyer, & Kinzelbach, 2002) and thereby also infiltration and the rate of substrate provision and associated residence time distributions (Aubeneau et al., 2016; Caruso et al., 2017). This dynamic dependence of porosity upon biomass and of biomass growth rates on porosity generates a complex, self-limiting bottom-up feedback effect whereby microbial biomass limits the flow that initially supported its growth.

In our work, we hypothesize that the impacts of these internal bottom-up feedback on seasonal rates of biogenic gas production and microbial growth will vary with the physical, hydrological, and ecological conditions of the riverbed at the beginning of the growing season (Marmonier et al., 2012; Power, 1992; Power et al., 2009; Power et al., 2008; Zarnetske et al., 2011). In Mediterranean climates, for example, where mild wet winters and long hot dry summers are common (Bonada & Resh, 2013; Inman & Jenkins, 1999), this corresponds with the dry, low river flow summer period after the winter and spring wet season. Mediterranean climates occur around the world between 30 and 40° latitude and are typically found on the western edges of continents (Deitch et al., 2017). River flow variability during the wet season in Mediterranean regions (of which California is included) from intense precipitation events such as atmospheric rivers (Dettinger et al., 2011) represents an external top-down impact that can shape riverbed geomorphology (Aalto et al., 2003; Kondrashov, 2005), sediment type (Andrews & Antweiler, 2012; Cayan et al., 1999; Mutiti & Levy, 2010), and grain size variability (Karwan & Saiers, 2012) at the beginning of the summer dry season. Since seasonally dry climates are characterized by tremendous variability in wet season conditions, a wide suite of potential summer initial sediment conditions and hyporheic behaviors are possible (Vico et al., 2015).

DN is one such hyporheic process where great variability has been observed across all sediment conditions. As pointed out by Harvey et al. (2011) and Lansdown et al. (2012), studies on the role of streambed sediments on DN rates often provide inconsistent, often conflicting rates as a function of grain sizes. Conflicting results range from reports of higher overall respiration rates in coarse sediments (B. N. Harvey et al., 2011; Hou et al., 2017) and greater DN in coarse gravels in the top 10 cm along stream riffles (Lansdown et al., 2012) to reports of lower DN in coarse grain sizes (Garcia-ruiz et al., 1998) and greater microbial activity in gravels paired with lower DN rates (Dodds et al., 1996). A variety of geomorphic, hydrodynamic, climatic, and sediment conditions have emerged as factors jointly controlling DN rates, yet the fundamental role of sediment structure in controlling respiration rates is missing (Findlay, 1995; J. W. Harvey et al., 2013; Ritz et al., 2018).

Summer dry conditions following wet winters represents a period in which Mediterranean rivers often transition from being gaining to losing rivers (Crosbie et al., 2014; Lamontagne et al., 2013; Oyarzún et al., 2014; Sapriza-Azuri et al., 2015), particularly as groundwater levels decline (Lavers et al., 2015). As drying progresses, losing rivers can further transition from being hydraulically connected to the groundwater through a continuously saturated zone to being disconnected from the underlying aquifer by an unsaturated zone (Lamontagne et al., 2013; A. M. McCallum et al., 2013; Rivière et al., 2014; Su et al., 2007; Treese et al., 2009). Water table fluctuations associated with anthropogenic pumping and hydrological perturbations can induce oscillations between conditions of gaining and losing (Baratelli et al., 2016; Pryet et al., 2015), and disconnection/reconnection that may limit or enhance infiltration patterns and nutrient supply supporting increased reactive efficiencies within the hyporheic zone (Trauth & Fleckenstein, 2017).

In this study, we develop and test a model that can simulate joint riverbed biological-physical feedback. We use the model to explore how variations in groundwater levels, antecedent hydrological conditions, initial riverbed sediment characteristics, and dissolved organic carbon (DOC) delivery influence nutrient transformations in the hyporheic zone and resulting storage or release of C and N in biomass and biogenic CO_2 and N_2 to the atmosphere to quantify the hyporheic controls on NEP (Figure 1, R_{h2}). We hypothesize that the initial riverbed sediment characteristics, specifically hydraulic conductivity (K_c) and porosity (Φ), exert a major control on hyporheic bioclogging and C and N consumption through bottom-up feedback, while the prevailing hydrology represents the main top-down control on C and N export in the form of CO_2 and N_2.

The remainder of this study is organized as follows. In section 2, we describe our assumptions, methods, and modeling framework. Section 3 describes our modeling results for an ideal, nonlimiting system. The modeling results are quantified by assessing hyporheic biogenic gas production and then release of those same

gases to the river which represents the R_{h2} term in Figure 1. To the author's knowledge, this is the first study to quantify the hydrological and sediment controls on the hyporheic component of heterotrophic respiration that includes microbial biomass growth as a physically constraining feedback. Section 4 then describes the role of the hyporheic zone in river systems.

2. Methods

In this study we compare infiltration, nutrient consumption, microbial growth, subsurface storage of C and N, and gas production feedback across multiple scenarios of hydrological and riverbed sediment conditions using a 1-D model setup of the hyporheic-aquifer zones (Figure 1). We analyzed these feedback mechanisms within the context of a seasonally dry semiarid gravelly river that is periodically experiencing river-aquifer connection dynamics and that is prone to prolonged periods of drought with superimposed fluctuations from a dynamic water table and groundwater pumping. These dynamics were investigated using bioclogging, infiltration, and pumping data from the Wohler Riverbank Filtration Site located along the Russian River, California, USA, as a representative Mediterranean site (study area and data collection described in supporting information S1; Ulrich et al., 2015). In this section, we describe model development and the range of water table and riverbed sediment characteristics imposed in our numerical study.

2.1. Model Development

One-dimensional models representing vertical flows between the Russian River and the underlying aquifer were developed using the MIN3P reactive transport code with the two-layer sediment structure representing simple heterogeneity shown in Figure 1 (Mayer et al., 2002). MIN3P is a finite volume numerical code for variably saturated subsurface flow and multicomponent reactive transport. A 25 m vertical model domain was discretized with variable spacing (0.01 m–0.1 m) and two sediment layers representing the riverbed clogging layer and underlying aquifer layer where K_c and K_a refer to saturated hydraulic conductivity of the riverbed clogging layer and aquifer layer, respectively (Figure 1). We chose this simple, two-layer heterogeneity model to allow the river and aquifer to undergo disconnection following a losing-connected, losing-transitional, and losing-disconnected sequence with periodic switches between losing and gaining conditions (Brunner, Simmons, & Cook, 2009; Irvine et al., 2012). Within each model layer, we did not include within-layer heterogeneity such as sublayers with different hydraulic properties or geostatistical sediment distributions, and we assumed homogeneous hydraulic properties for each of the two layers. We acknowledge that real systems have tremendous heterogeneity even within seemingly homogeneous sediment types, and river dynamics may allow stratigraphic sequences with multiple and alternating high- and low-permeability layers. The potential implications of this are multiple "bottlenecks" along the flow paths and development of preferential flow paths that significantly influence flow and solute transport (Fox et al., 2016; Hatch et al., 2010; Tang et al., 2015; Tonina et al., 2016; Zhou et al., 2014).

A 1-D modeling approach introduces major assumptions concerning the dominant direction of flow since this is by definition unidirectional at any point in time and space and neglects multidimensional flow paths intrinsic to hyporheic systems. In most subsurface systems, flow is not 1-D but instead a complex distribution of flow paths and directions that have wide residence time distributions at varying depths (Fox et al., 2016; Sawyer & Cardenas, 2009) and bidirectional flow paths that are also intrinsically 3-D (Trauth et al., 2015). We chose to use 1-D models as a preliminary exploration of the role of microbial populations on biogeochemical cycling and to keep scenario-based complexity manageable for representing rivers where dominant seepage directions are vertical rather than horizontal (Fleckenstein et al., 2006; Kalbus et al., 2009).

Reactive transport conditions included pore space microbial aerobic respiration (AR), NI as an additional source of nitrate, and pore space microbial DN. Modeling frameworks exist for microbial species across many different terminal electron-accepting processes in the redox sequence (Azizian et al., 2017; Canfield et al., 1993; Thullner et al., 2007). Using dual-Monod kinetics, microbial growth was specified as a function of the concentration of nutrient substrates and the concentration of microbial mass already in the system (Murphy & Ginn, 2000). We chose to use dual-Monod kinetics to allow the dependence of reaction rates on biomass, O_2, DOC, and NO_3^- concentrations. This method assumes a single-step approach when transforming organic carbon to dissolved inorganic carbon and aerobic biomass (hereafter referred to as AR biomass) assuming a microbial yield (y) of 0.33 in equation (1) for AR (y ranges between 0.1 and 0.6 for both AR and DN)

(Molz et al., 1986; Thullner, Zeyer, & Kinzelbach, 2002; Zarnetske et al., 2012). In this case, the molar coefficient $Y = 1$ produces the yield $y = Y/(2 + Y) = 0.33$:

$$(2 + Y)CH_2O + 2O_2 \leftrightarrow 2CO_3^{-2}(aq) + 4H^+ + YCH_2O_{ARbio} \quad (1)$$

Organic carbon is oxidized in this reaction and assumed to be in dissolved form. Biomass growth is represented through the oxidation of organic carbon by aerobes and is expressed as the biomass term in equation (1). Aquatic organic matter with a generalized formula representing DOC was represented by the ratio C_1:H_2:O_1 (Matsunaga et al., 1993). We used a biomass density of 0.8 g cm^{-3} dry mass/wet volume (800 kg m^{-3}) which is within the range of reported densities (0.1–1100 kg m^{-3}) for microorganisms including bacteria, algae, fungi, and extracellular polymeric substances (Ezeuko et al., 2011; Kildsgaard & Engesgaard, 2001; Rockhold et al., 2005; Rosenzweig et al., 2014; Thullner, 2010; Thullner et al., 2004). Carbonate equilibrium is assumed as a function of pH:

$$CO_3^{-2} + 2H^+ \leftrightarrow H^+ + HCO_3^- \leftrightarrow H_2CO_3 \leftrightarrow CO_2(aq) + H_2O \quad (2)$$

Biomass growth through the anaerobic oxidation of organic carbon by denitrifying microorganisms (referred to as anaerobic biomass or DN biomass) is considered through the following equation where nitrate is the electron acceptor and the microbial yield is 0.17 (Kildsgaard & Engesgaard, 2001):

$$(5 + Y)CH_2O + 4NO_3^- + 4H^+ \leftrightarrow 5CO_3^{-2}(aq) + 10H^+ + 2N_2(aq) + 2H_2O + YCH_2O_{DNbio} \quad (3)$$

Aerobic NI was included to represent an additional source of nitrate:

$$NH_4^+ + 2O_2 \leftrightarrow NO_3^- + H_2O + 2H^+ \quad (4)$$

To allow microbially induced reduction of riverbed K_c and Φ during the simulation, we implemented a novel bioclogging feedback mechanism in the MIN3P code using the bioclogging "Colony" constitutive model (Thullner, 2010). The Colony model assumes an aggregated form of biomass in the pore space. We implemented the permeability and porosity feedback in the MIN3P numerical code with published parameters to allow the feedback between biomass growth and K_c and Φ parameter updates at each time step during the entire model run (Thullner, Mauclaire, et al., 2002; Thullner, Zeyer, & Kinzelbach, 2002). Conceptually, as the biomass grows, the physical size of the pore space declines, which reduces K_c and Φ. Biomass accumulation was represented in the MIN3P model as a volume fraction of biomass occupying the pore space allowing a new Φ and the new K_c at each time step. We chose the Colony model based on field measurements of biomass growth and simulated infiltration responses to the Colony model fit to the bioclogging and infiltration field data (supporting information S1) (Newcomer et al., 2016). To the author's knowledge, allowing microbial biomass to grow and provide a feedback to sediment parameters is not yet common in modeling approaches. We ran two biomass groups—allowing simulations with and without this feedback (hereafter abbreviated "With Bio Feedback" and "Without Bio Feedback"), to test the impact of microbial growth on flow and transport and to provide an estimate of how much this modeling choice impacts respiration estimates.

2.2. Boundary Conditions, Initial Conditions, and Model Parameterization

Boundary and initial conditions are presented in Table 1. Large dissolved CH_2O (DOC) concentrations (0.6 and 1.6 mmol/L) were chosen for the top boundary condition of the model. Our two choices of top DOC boundary conditions are presented in Table 1 and represent previously published DOC values (0.6 mmol/L) (Trauth et al., 2014) and a maximum case representing highly labile autochthonous sources from benthic river systems (1.6 mmol/L) (Acuña et al., 2004; ElBishlawi & Jaffe, 2015; Flipo et al., 2004; Flipo, Rabouille, et al., 2007; Kaplan & Bott, 1982, 1989; Mann & Wetzel, 1995; Wyatt et al., 2012). Bottom DOC concentrations were selected from Rivett et al. (2008). Other species included in the model and reported in Table 1 were dissolved O_2 (DO), nitrate (NO_3^-), and ammonia (NH_4^+). DO concentrations for the surface were taken from average Russian River DO measurements (morning, 9 mg/L; afternoon, 13 mg/L) and bottom concentrations taken from reported groundwater far-field conditions (1–11 mg/L) (Kolbjørn Jensen et al., 2017). Nitrate (NO_3^-) values were chosen for the top (5 mgNO_3^-/L) and bottom (1 mgNO_3^-/L) condition based on river and groundwater measurements (USGS Guerneville Station #11467000). Top values for NO_3^- are low compared with other studies (Sudduth et al., 2013). While groundwater NO_3^- contamination is a common condition of growing concern around the world (Flipo, Jeannée, et al., 2007; Seitzinger et al., 2006; Spalding & Exner, 1993),

Table 1
Flow and Reactive Transport Boundary Conditions Used in the 1-D Model

	Boundary type		Hydraulic head	Concentrations				
	Flow	Solute		DOC (mg C/L, mg CH_2O/L, mmol/L)	DO (mg/L, mmol/L)	NO_3^- (mg NO_3^-/L, mmol/L)	NH_4^+ (mg NH_4^+/L, mmol/L)	Temperature (°C)
Top	Head	[a]Free exit/mass flux[a]	1 m	8–20, 20–50, 0.6–1.6	11, 0.34	5, 0.08	1.5, 0.09	20
Bottom	Variable head	[a]Free exit/mass flux[a]	See Figure 3	0.4, 1, 0.03	7, 0.2	1, 0.016	1, 0.06	20
Initial conditions			10.2 m (neutral)	0.2, 0.5, 0.017	4, 0.13	1, 0.016	1, 0.06	20

Note. DOC = dissolved organic carbon; DO = dissolved O_2.
[a]The bottom solute boundary condition changes from a Neumann (free exit flux condition) boundary when the flow is leaving the domain to a Cauchy (mass flux based on concentration) boundary when flow is entering the domain.

we simplify our model to the scenario where groundwater NO_3^- contamination is not present. We acknowledge that this assumption may change the dynamic of DN in gaining rivers when the NO_3^- source is groundwater; however, we chose this condition to better constrain modeled sources and sinks to the river only. Ammonia (NH_4^+) concentrations were chosen from measured river concentrations at USGS Guerneville Station #11467000 and assumed for the lower boundary based on measurements of urban impacted rivers (Vilmin, Flipo, Escoffier, & Groleau, 2016).

Dual-Monod maximum growth rate coefficients for AR and DN were 1E−4 $\frac{M_{DOC}}{M_{O_2} M_{bio} s}$ and 1E−5 $\frac{M_{DOC}}{M_{NO_3} M_{bio} s}$ and were chosen from published ranges (M = mol/L of each species and s = seconds) (Rosenzweig et al., 2014; Thullner, Zeyer, & Kinzelbach, 2002; Trauth et al., 2015). NI was included with a maximum specific growth rate coefficient of 1E−4 $\frac{M_{NH_4}}{M_{O_2} s}$. Ranges of NI rate coefficients can be found in the literature (Admiraal & Botermans, 1989; Aissa-Grouz et al., 2015; Raimonet et al., 2015; Sheibley et al., 2003; Strauss et al., 2004). Half-saturation constants for O_2 were (3.125E−6 M), CH_2O (1.0E−4 M), and NO_3^- (8.064E−6 M). Aqueous and gaseous diffusion constants were 2E−9 and 2E−5 $m^2\ s^{-1}$, respectively. Lysis of biomass (cell decay) and turnover back to DOC was given the rate constant of 1E−7 s^{-1}. These parameters were chosen from a range of published values (Dupin et al., 2001; Rockhold et al., 2005; Rosenzweig et al., 2014; Samsó et al., 2016; Thullner et al., 2005).

Advective-diffusive transport was simulated for dissolved solutes and dissolved gases, while for the gaseous phase, only diffusive transport was considered. Gas phase advection was neglected for our selected flow and transport conditions because dissolved gas concentrations never reached solubility and no formation of gas bubbles or gas continuums had to be considered. Gas phase advection could occur through continuous pressure gradients along the continuous gas phase or by bubble formation and movement within the liquid. Lacking this gas phase advective pathway, however, introduces major assumptions about gas storage in subsurface systems. In this model, gases cannot escape to the atmosphere under losing conditions or by 2-D lateral flow, and this has implications for natural systems where the gaseous-phase advection may move gas in opposite directions to water flow (Cuthbert et al., 2010; Rockhold et al., 2005; Yarwood et al., 2006). Carbonate mineral precipitation and dissolution was also included, but this was negligible relative to the formation of biomass species. Each simulation covered 1,000 days with a minimum time step of 1E−8 days and maximum time step of 0.025 days, with each time step scaling to capture the reaction kinetics adequately.

2.3. Riverbed Sediment Characteristics and Their Control on Subsurface Flow

In Mediterranean climates, weather-controlled river flow conditions shape riverbed grain size distributions through scouring benthic sediments during energetic flows and depositing sediments during low flow conditions (Vilmin et al., 2015). We conceptualized the impact of river flow conditions on the numerical model by setting different combinations of the initial riverbed layer sediment conductivity K_c and porosity Φ at the start of each simulation (i.e., Gray et al., 2015a, 2015b; Marcarelli et al., 2015; Mutiti & Levy, 2010; Schälchli, 1992). We identify several sediment classifications having distinct porosity and hydraulic conductivity distributions associated with a simple conceptual model of semiarid riverbeds with gravelly, poorly sorted, highly heterogeneous sediments. We assume that more energetic river flow conditions will generally lead to larger Φ, more uniform grain size distributions, coarse packing, and larger K_c (i.e., Mutiti and Levy, 2010), whereas hydrograph falling limbs and less energetic river flow conditions will lead to smaller Φ, poorly sorted grain size distributions, fine packing, and smaller riverbed K_c (Figure 2) (W. Chen et al., 2013; Kamann et al., 2007; Leonardson, 2010; Marcarelli et al., 2015). The complexity associated with sediment texture, sorting, porosity, conductivity, and flow conditions have been extensively reported (Aalto et al., 2003; Beard & Weyl, 1973; Boadu, 2000; X. Chen et al., 2008; Inman & Jenkins, 1999; Rosenberry et al., 2012; Shepherd, 1989; Slatt, 2006; Sneider, 1987).

Six values of riverbed K_c (2.0E−6, 5.0E−6, 9.0E−6, 1.3E−5, 2.0E−5, and 6.0E−5 m/s) were used. Values of riverbed K_c were chosen at the higher end of those reported for semiarid riverbed sediments (1.0E−6 to 1E0 m/d or 1.0E−11 to 1.0E−5 m/s) which represent poorly sorted heterogeneous cobbles and gravels (Aqtesolv, 2016; Geotechdata, 2008; Taylor et al., 2013). We chose two values for aquifer conductivity K_a (1.0E−4 and 3E−4, m/s) based on previous estimates for our site (Su et al., 2004; Zhang et al., 2011). The choice of K_a then constrained our choices for K_c because we had to ensure that two criteria were met: (1) modeled seepage generally matched that found at the field site (Figure S2c), and (2) to fulfill the criteria

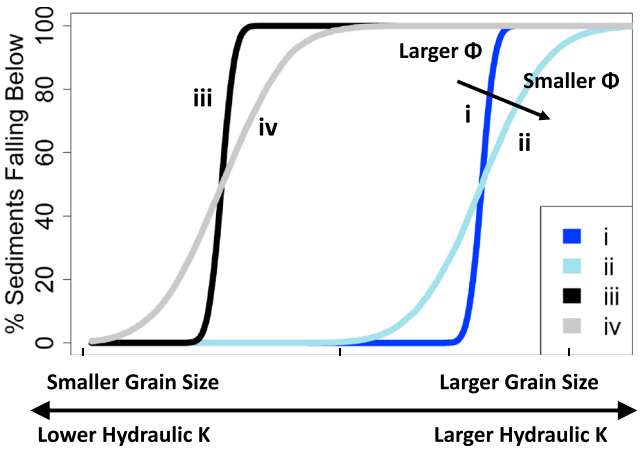

Figure 2. Sediment grain size distributions inspired by published sediment packing arrangements and degree of heterogeneity that contribute to complex Φ and K_c end-members (Kamann et al., 2007).

for disconnection (Brunner, Cook, & Simmons, 2009) since evidence for disconnection was observed at the site from infiltration and geophysical data (Newcomer et al., 2016; Ulrich et al., 2015). Four values of riverbed porosity Φ (0.17, 0.21, 0.28, and 0.34) were tested. A total of 96 parameter combinations was used (2 DOC, 6 K_c, 4 Φ, and 2 K_a, $2 \times 6 \times 4 \times 2 = 96$).

We classify the end-members of the sediment parameters of riverbed hydraulic conductivity (K_c) and riverbed porosity (Φ) into categories that are conceptually representative of current and antecedent hydrological conditions (Figure 2). We define our end-members by the four possible combinations of maximum/minimum K_c and maximum/minimum porosity and conceptually link these to river flow regime. The hydrogeologic end-members are as follows:

1. *High* (Figure 2, line i. A high-K_c and high-Φ sediment structure (K^+ Φ^+). This end-member classification is included to represent sediment characteristics of rivers with consistently high flows. High flow is often accompanied by enhanced sediment scour (Petticrew et al., 2007; Vilmin et al., 2015) and where additional spring storms continually loosen fine sediment leading to high riverbed conductivities and porosities.
2. *Medium* (Figure 2, line ii. A high-K_c and low-Φ case (K^+ Φ^-). This end-member is included to represent higher than average river flows which contribute to enhanced sediment scour, and larger grain sizes, while dry spring conditions contribute to fine sediment deposition that increase the standard deviation of grain sizes leading to lower Φ, and the potential for periphyton biomass to establish on the riverbed (Flipo, Rabouille, et al., 2007).
3. *Moderate* (Figure 2, line iii. This end-member represents low-K_c and high-Φ sediment characteristics (K^- Φ^+) with a narrow grain size distribution and lower average grain sizes shifted toward sands/silts instead of gravels. These sediments may occur for lower than average river flow and a consistent number of spring storms to achieve well-sorted sediments. Frequent small storms can maintain good sorting of sandy sediments, which allow porosities to remain high, while conductivities are low because of the shift in overall grain size distribution to small sediments.
4. *Low* (Figure 2, line iv. A low K_c-low Φ sediment structure (K^- Φ^-). Lower than average river flow conditions contribute to reduced total sediment scour; the lack of winter and spring storms lead to lower porosities from enhanced sediment deposition, poorly sorted sediments, greater heterogeneity in sediment grain size distributions, and lower conductivities.

2.4. Water Table Characteristics

Water table fluctuations from weather-controlled hydrological and engineered perturbations were included to represent the main control on seepage flow direction and the length of time water flows down (losing) versus up (gaining). Five different water table cases representing different seasonal perturbations and human-based controls on hydrology are simulated (Figure 3). These represent the river-aquifer conditions found in the center of the stream and include

1. *Dry*—Baseline losing case *without* fluctuations. This is conceptualized as a dry period where a water table drops and never recovers the original position. In this case, the river and aquifer undergo indefinite disconnection, and the flow direction is always downward.
2. *Fluctuating*—A neutral wet-dry seasonal cycle where the water table rises and falls seasonally *with* superimposed shorter-term fluctuations. The river and aquifer occasionally undergo disconnection and reconnection where flow direction switches from gaining→losing→gaining.
3. *Average*—A water table that rises and falls seasonally *without* short-term fluctuations. This helps to isolate the effects of the fluctuations on redox-controlled memory effects in sediment strata as in the Fluctuating case.
4. *Wet*—The water table rises and falls seasonally, but because of greater than average wet conditions, the river is more often gaining with short periods of dry losing-disconnected conditions during the summer.

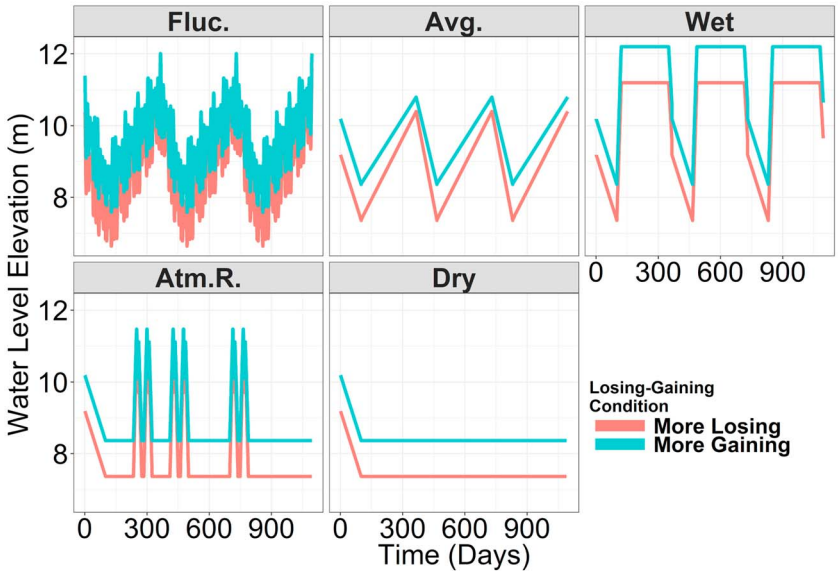

Figure 3. Water table decline over time with superimposed fluctuations. The water table can be more gaining or more losing, with large and small fluctuations superimposed. The water table position controls the direction of flow from the groundwater to the river (gaining) or from the river to the aquifer (losing). Neutral seepage conditions occur at a water table elevation of 10.2 m.

5. *Atmospheric river*—Atmospheric rivers are long narrow plumes of concentrated water vapor that contribute to extreme precipitation and flooding events around the world (Waliser & Guan, 2017), with an average of 1–10 events each year in California (Dettinger et al., 2011). We represent this as a dry losing-disconnected period punctuated by atmospheric rivers stimulating short periods of transitional losing→gaining conditions, which represent the impact of storm events, and resulting bank storage on river gaining conditions (J. L. McCallum & Shanafield, 2016).

Among all cases, we also tested on average more losing or more gaining conditions (Figure 3). Since infiltration rates are a function of the hydraulic gradient, lower water tables lead to faster infiltration rates, and more shallow water tables lead to slower infiltration rates. We tested these cases with the hypothesis that lower water tables generally limit the number of reversals in flow direction from losing→gaining and allow transport rates to generally be greater than reaction rates leading to a reaction-limited system. Conversely, we hypothesize that more shallow water tables generally allow a greater number of flow reversals past the neutral point (10.2 m), limit transport rates relative to reaction rates, and, on average, allow the system to be transport limited.

We simulated daily and seasonal frequencies of water table variations to represent natural seasonal and human-based effects on regional and local water levels (i.e., high flows, pumping, dam effects, etc.). For the Fluctuating case, we used stochastic water level fluctuations to describe the variability in frequency and magnitude. The approach and parameters used to construct the water table scenarios were based on a Fourier analysis of the dominant pumping frequencies and are described in supporting information Texts S1–S3 (Plant, 2012). We provide supporting information R code in Code S1 that reproduces the stochastic water levels as from the pumping data set provided in supporting information Data Set S1. A total of 1,000 water table cases was simulated (5 water table groups × 2 more losing/more gaining cases × 100 stochastic variations). Introducing stochastic water level fluctuations on the daily and seasonal time scale not only perturbs the model in a way that mimics natural and human-based effects but also introduces feedback in subsurface regions that experience periods of overlap between aerobic/anaerobic and wet/dry periods. In this model setup, we neglected any variation in river level conditions to simplify model complexity. River water levels would certainly impact the timing and strength of gaining and losing conditions, and we suggest that this is a line of inquiry for future model-based studies.

All parameter, sediment, and water table groups were run first with the biomass module implemented and then repeated without biomass growth to determine how the bioclogging-parameter feedback

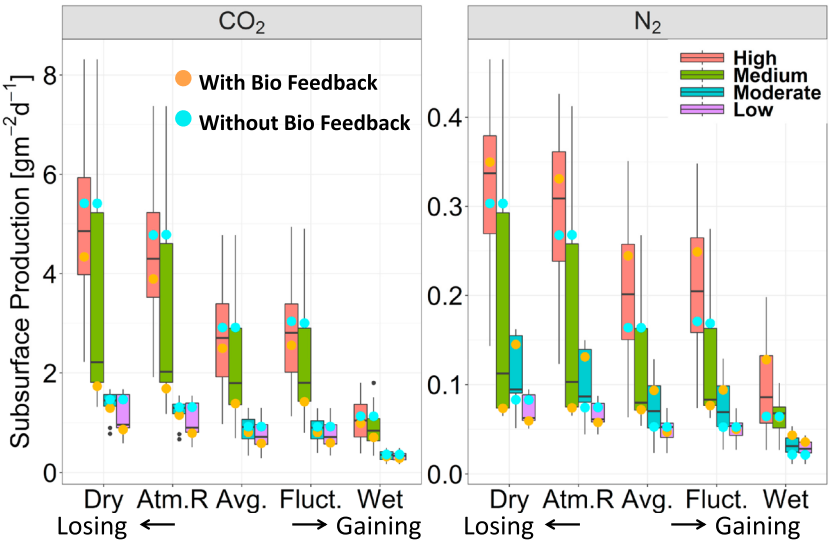

Figure 4. CO_2 and N_2 production as a function of the hydrogeologic streambed end-members defined above (High, Medium, Moderate, and Low), and water table cases (Dry, Atmospheric River, Average, Fluctuations, Wet). Blue and orange points show averages for the cases that allowed and did not allow pore space aerobic respiration and denitrification biomass growth feedback, and black dots show outliers.

mechanism can contribute to uncertainty in AR and DN when neglected. The 96 parameter groups × 2 biomass groups × 1,000 water table simulations provided 192,000 total MIN3P simulations and were conducted on the UFZ EVE cluster and the LBNL Lawrencium cluster. Total infiltration fluxes; biomass growth; carbon consumption from AR and microbial DN, CO_2, and N_2 gas subsurface production; C and N subsurface storage; and CO_2 and N_2 release to the river were extracted from all 1-D models and compared across the different sediment characteristics and water table groups.

3. Results

3.1. CO_2 and N_2 Production in the Hyporheic Zone

Production of CO_2 ($g/m^2/d$) in the subsurface as a product of AR and DN reactions is shown across the water table perturbation groups ranging from more losing to more gaining river conditions (Figure 4). In general, CO_2 production is always 2–3 times greater than N_2 production for all sediment groups and generally increases with sediment Φ and K_c. In the Dry case, CO_2 production ranged between 1 and 7 $g/m^2/d$, while in the Wet case CO_2 production ranged between 0.5 and 1 $g/m^2/d$. Average and Fluctuating conditions facilitating periods of limited nutrient fluxes appear to limit CO_2 and N_2 production.

Initial riverbed K_c and Φ end-members also strongly control CO_2 and N_2 production within the water table groups. Cases with High (K^+ Φ^+) and Medium (K^+ Φ^-) sediment classification are associated with the most biogenic gas production—an effect that is similar across all water table models. High initial Φ sediments (High) and low initial Φ sediments (Medium) show vastly different mean CO_2 production (4.8 versus 2.1 $g/m^2/d$, respectively). Cases with the Low (K^- Φ^-) and Moderate (K^- Φ^+) sediment classification do not show the same variation across the water table conditions. Across all water table models, CO_2 and N_2 production is quite limited for initially Low and Moderate sediments, which have the lowest K_c values. Regardless of the initial Φ value, these sediment classes have limited substrate provisions to deeper sediments and are the least productive in general.

3.2. CO_2 and N_2 Release From the Hyporheic Zone to the River

While CO_2 production in the hyporheic zone is highest for the Dry case with High sediment characteristics, the portion of CO_2 and N_2 that can reemerge back to the river also varies with sediment type and water table case (Figure 5). Release of gases from the hyporheic zone occurred from a reversal in seepage direction from losing→gaining. Percentages of biogenic gas released to the river relative to what was produced in the hyporheic zone are shown above the bars in Figure 5.

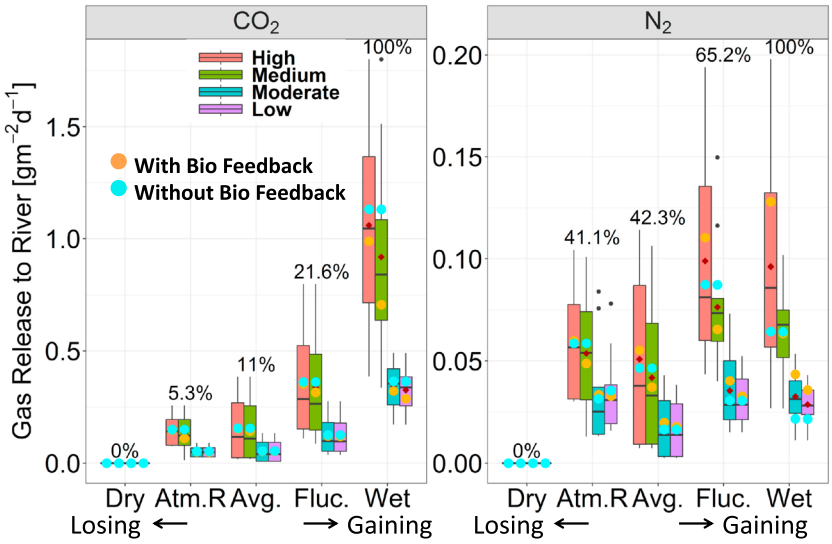

Figure 5. Release of CO_2 and N_2 to the river grouped by water table fluctuation case. Percentages refer to the average percent of gas released to the river relative to the total gas produced in the hyporheic zone. Blue and orange points show averages for the cases that allowed and did not allow pore space aerobic respiration and denitrification biomass growth feedback, and black dots show outliers.

As expected, Dry, more losing cases with indefinite water table declines contribute little, if any, to river hyporheic zone respiration NEP metrics (R_{h2} term in Figure 1), contributing between 0 and 11% of gases produced. Gaining rivers (Wet or Atmospheric river cases) allowed the greatest fraction of CO_2 and N_2 production to return to the river as an external flux. Gaining cases contributed between 20 and 100% of the gases produced. Atmospheric river cases were the most efficient, exporting 41% of the N_2 produced in the subsurface during four to five "storm events" which allowed gaining conditions only 6% of the total time period. Fluctuating cases were the second most efficient, exporting on average 65% of the N_2 produced during 10% of the total time period. Even though Wet cases produced less biogenic gas compared with the Dry case (Figure 4), most of the CO_2 and N_2 produced eventually returned to the river when provided with a hydrological opportunity. Values of hyporheic zone respiration are comparable to results presented in studies with measurements and estimates of hyporheic zone rates ranging between 1 and 2 g/m^2/d of CO_2 (Hotchkiss et al., 2015), 0.23–0.37 g/m^2/d of CO_2 (Vilmin, Flipo, Escoffier, Rocher, & Groleau, 2016), and 0.1–0.4 g/m^2/d of N_2 (J. W. Harvey et al., 2013).

Coupling between the overarching hydrological/seasonal fluctuating conditions and the sediment characteristics is also evident in the results for biogenic gas release. Cases with High ($K^+ \Phi^+$) and Medium ($K^+ \Phi^-$) sediments were found to release, on average, a greater percentage of biogenic gas production relative to Low ($K^- \Phi^-$) and Moderate ($K^- \Phi^+$) sediment classes. In the cases that allow fluctuations (Atmospheric river, Average, and Fluctuating) along the spectrum of infrequent to frequent fluctuations, N_2 released back to the river was generally greater as a percentage of production relative to CO_2.

3.3. Biomass Growth and Carbon Storage in the Hyporheic Zone

We define the "biomass volume" as the amount of pore space within the bulk riverbed sediment that is occupied by biomass and is a dimensionless value similar to porosity. With sufficient nutrient supply, biomass grows until it reaches the maximum volume, which is equal to the porosity. When biomass volume equals the porosity, then the pore space is completely occupied (biomass volume/porosity = "biomass volume fraction" = 1 or "biomass pore space percentage" = 100% when full). Average biomass volume from AR and DN is shown in Figure 6a with depth, averaged across the water table cases and all DOC values. Most of the biomass volume for both AR and DN is found within the top 10 cm of the sediment column leading to the development of a microzone that facilitates the growth of both AR and DN microbes. We discuss the significance of this microzone in section 4.

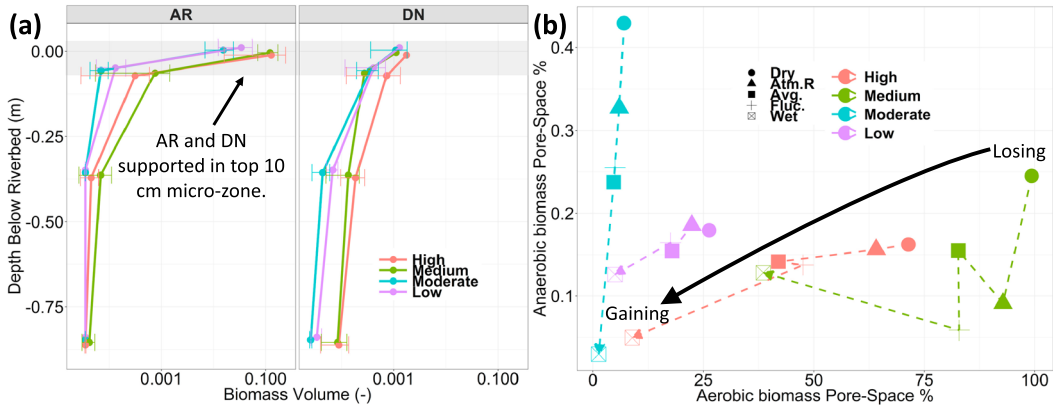

Figure 6. (a) Biomass volume (—) from aerobic respiration (AR) and denitrification (DN) with colored bars showing the average and standard deviation among all stochastic water table cases and dissolved organic carbon (DOC) boundary condition values. The gray region at the top highlights the top 10 cm microzone. (b) Average biomass pore space percentage (percent of the pore space that is full) separated by sediment type and water table fluctuation case. Biomass values in (b) are taken from the top 10 cm of the riverbed sediment at day 365 for K_a = 1E−4 m/s and DOC = 0.6 mmol/L.

Comparing AR and DN biomass pore space percentage after 1 year reveals a wide suite of microbial behaviors (Figure 6b). Water table cases clearly represent a significant control on the total amount of biomass that can grow in the pore space. Dry water table cases, with highly losing conditions, represent the environment in which maximum AR and DN biomass can grow for all sediment types. Biomass from DN contributes 1 to 2 orders of magnitude less to the clogging of the pore space than biomass from AR.

Sediment type reveals strong controls on the proportion of DN versus AR biomass based on K_c and Φ combinations. When comparing the high K_c group (High (K^+ Φ^+) and Medium (K^+ Φ^-) end-members) to the low K_c group (Low (K^- Φ^-) and Moderate (K^- Φ^+)), AR biomass is larger for high K_c sediments (Figure 6b). High and Medium sediments generally clog >50% of the pore space. Within the high K_c group, smaller porosity sediment (Medium) has a larger percent of AR biomass compared with the high porosity sediment. The Moderate end-member shows enhanced DN biomass relative to other sediment groups across all water table cases. Enhanced DN in these sediments is not surprising given that any opportunity for NI to proceed forward (in competition with AR for O_2) would produce additional NO_3^- used for DN and additional biomass growth.

Total DOC fate between biomass, gas production, and unreacted DOC in the subsurface is shown across sediment hydrogeologic end-members and grouped by water table scenario in Figure 7. Total DOC storage as biomass and dissolved gases in the subsurface as a percent of influx (purple line) varies quite significantly between the water table scenario groups and shows an order of magnitude greater total storage of incoming DOC for Dry versus Wet cases (Figure 7a). Dry cases, in general, show larger C storage in biomass alone compared with the other water table groups. Figure 7b shows the percent distribution of DOC, and porosity-controlled C storage trends corroborate CO_2 release—high Φ sediments store less net C as biomass but contribute to greater net AR/DN gas production. Low Φ sediments show a greater proportion of DOC remaining as biomass.

3.4. Reaction Rates of AR and DN

Spatially averaged (over the entire model domain) AR, DN, and NI reaction rates (mol/m^2 riverbed/d) are shown in Tables 2 and 3 as Early and Late time averages (day 0 to day 100 and day 365 to day 730) during the model simulations for the sediment and water table cases. Values are averaged for each sediment end-member type (row averages), and for each water table case (column averages). The total average for all cases with and without microbial biomass feedback is also shown in the bottom corner. Average rates across all sediment and water table cases are shown in the Average column for cases With Bio Feedback shown in green, and Without Bio Feedback shown in red. In general, all reaction rates tended to decrease over time (DN: 0.046 → 0.030 mol/m^2/d, AR: 0.035 → 0.015 mol/m^2/d, NI: 0.02 → 0.008 mol/m^2/d); however, not all sediment end-members or water table groups followed this trend, and many sediment groups show increases in rates over time.

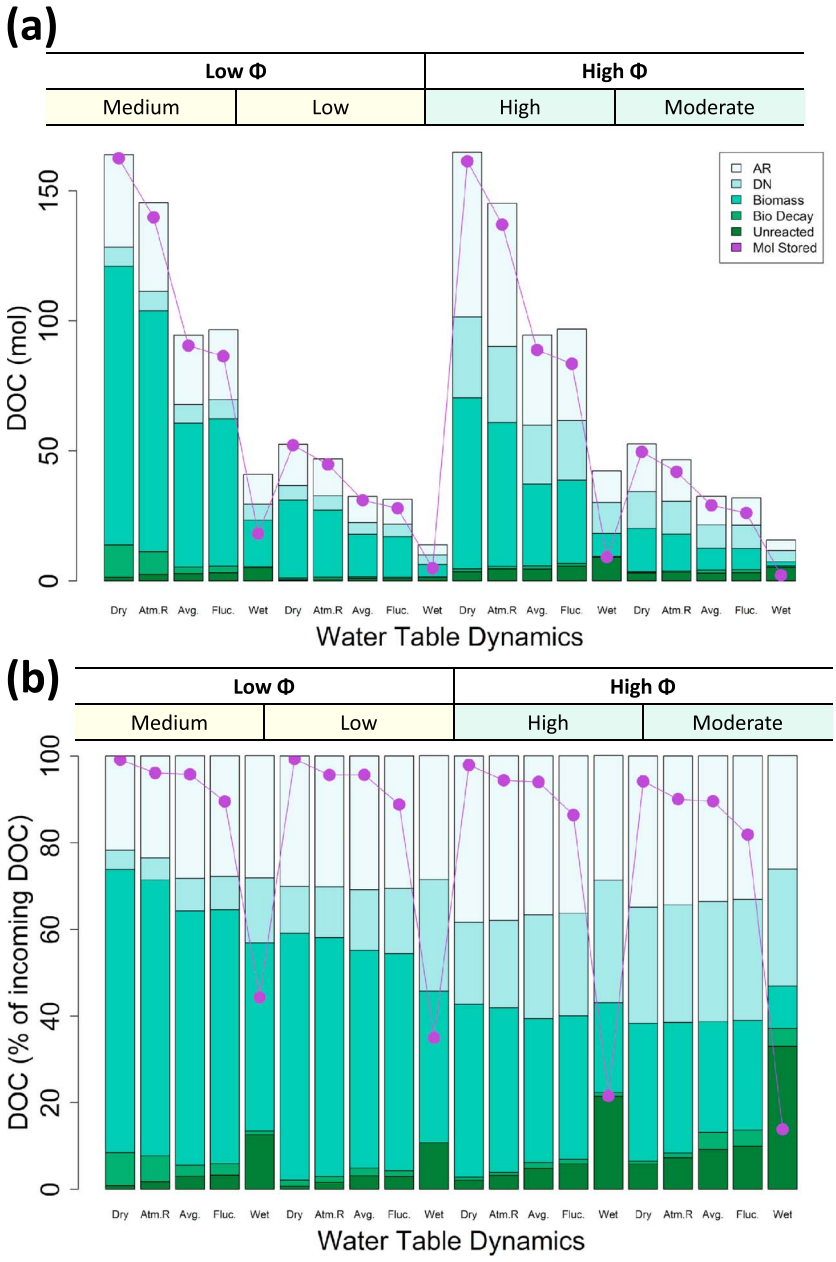

Figure 7. (a) Dissolved organic carbon (DOC) fate of subsurface aerobic respiration (AR) or denitrification (DN) produced gas, AR and DN biomass, biomass decay, unreacted DOC, and total DOC stored (purple dots) are shown as absolute values in moles. b) Percentage distribution of the total DOC fate in the subsurface (as a percent of total DOC influx) is shown across different sediment hydrogeologic classes and water table fluctuation scenarios. Results are shown for K_a = 1E−4 m/s at day 365.

Trends emerge between the water table scenarios and the sediment types that favor AR or DN at some point in time and show changes in these rates between early and late times. For example, sediments that support large initial transport rates relative to reaction rates (High sediment end-member) generally show large reaction rates at early times (averages of 0.051, 0.032, and 0.022 mol/m^2/d for DN, AR, and NI, respectively). In highly losing systems (Dry case), High sediments tend to show decreases in AR reaction rates over time (blue cell highlight early = 0.080, late = 0.046 mol/m^2/d), while DN reaction rates increase (orange cell highlight early = 0.077, late = 0.113 mol/m^2/d). When comparing the Fluctuating case to the other cases during early times, rates were always generally smaller for the Fluctuating case. In Medium sediments,

Table 2
Early AR, DN, and NI Mean Reaction Rates (mol/m^2 riverbed/d) and Standard Deviations for Each End-Member Sediment Classification and Water Table Case

Early times (day 0 to day 100)						
	Dry	Atmospheric rivers	Average	Fluctuations	Wet	Average
Denitrification rate (mol/m^2/d)						
High	0.077 ± 0.009	0.077 ± 0.009	0.077 ± 0.009	0.035 ± 0.043	0.077 ± 0.009	0.068 ± 0.016
Medium	0.074 ± 0.009	0.074 ± 0.009	0.074 ± 0.009	0.045 ± 0.043	0.074 ± 0.009	0.069 ± 0.015
Moderate	0.027 ± 0.003	0.027 ± 0.003	0.027 ± 0.003	0.014 ± 0.015	0.027 ± 0.003	0.024 ± 0.006
Low	0.026 ± 0.003	0.026 ± 0.003	0.026 ± 0.003	0.015 ± 0.015	0.026 ± 0.003	0.024 ± 0.005
Average	0.051 ± 0.006	0.051 ± 0.006	0.051 ± 0.006	0.027 ± 0.029	0.051 ± 0.006	0.046 ± 0.011 0.084 ± 0.019
Aerobic respiration rate (mol/m^2/d)						
High	0.080 ± 0.009	0.080 ± 0.009	0.080 ± 0.009	0.034 ± 0.045	0.080 ± 0.009	0.071 ± 0.016
Medium	0.031 ± 0.002	0.031 ± 0.002	0.031 ± 0.002	0.021 ± 0.014	0.031 ± 0.002	0.029 ± 0.004
Moderate	0.028 ± 0.003	0.028 ± 0.003	0.028 ± 0.003	0.014 ± 0.016	0.028 ± 0.003	0.025 ± 0.006
Low	0.016 ± 0.001	0.016 ± 0.001	0.016 ± 0.001	0.011 ± 0.006	0.016 ± 0.001	0.015 ± 0.002
Average	0.032 ± 0.004	0.032 ± 0.004	0.032 ± 0.004	0.014 ± 0.018	0.032 ± 0.004	0.035 ± 0.007 0.024 ± 0.005
Nitrification rate (mol/m^2/d)						
High	0.032 ± 0.004	0.032 ± 0.004	0.032 ± 0.004	0.014 ± 0.018	0.032 ± 0.004	0.028 ± 0.007
Medium	0.032 ± 0.004	0.032 ± 0.004	0.032 ± 0.004	0.019 ± 0.019	0.032 ± 0.004	0.030 ± 0.007
Moderate	0.011 ± 0.001	0.011 ± 0.001	0.011 ± 0.001	0.006 ± 0.007	0.011 ± 0.001	0.010 ± 0.002
Low	0.011 ± 0.001	0.011 ± 0.001	0.011 ± 0.001	0.006 ± 0.007	0.011 ± 0.001	0.010 ± 0.002
Average	0.022 ± 0.002	0.022 ± 0.002	0.022 ± 0.002	0.011 ± 0.013	0.022 ± 0.002	0.020 ± 0.005 0.000 ± 0.000

Note. Values are shown as means ± standard deviations for early times (day 0 to day 100) in the simulation. Averages are shown across the sediment (blue, row averages) and water table classes (brown, column averages). The total average for all cases is shown in the bottom right corner for simulations that include biomass growth feedback (green) and do not include biomass growth feedback (red). AR = aerobic respiration; DN = denitrification; and NI = nitrification.

Table 3
Late AR, DN, and NI Mean Reaction Rates (mol/m^2 riverbed/d) and Standard Deviations for Each End-Member Sediment Classification and Water Table Case

Late times (day 365 to day 730)						
	Dry	Atmospheric rivers	Average	Fluctuations	Wet	Average
Denitrification rate (mol/m^2/d)						
High	0.113 ± 0.014	0.093 ± 0.040	0.032 ± 0.005	0.015 ± 0.019	0.028 ± 0.004	0.056 ± 0.016
Medium	0.043 ± 0.005	0.045 ± 0.024	0.025 ± 0.003	0.011 ± 0.014	0.025 ± 0.003	0.030 ± 0.010
Moderate	0.035 ± 0.004	0.028 ± 0.012	0.009 ± 0.001	0.006 ± 0.006	0.009 ± 0.001	0.018 ± 0.005
Low	0.030 ± 0.003	0.023 ± 0.012	0.009 ± 0.001	0.005 ± 0.005	0.009 ± 0.001	0.015 ± 0.004
Average	0.055 ± 0.007	0.047 ± 0.022	0.019 ± 0.002	0.009 ± 0.011	0.018 ± 0.002	0.030 ± 0.009 0.050 ± 0.004
Aerobic respiration rate (mol/m^2/d)						
High	0.046 ± 0.001	0.039 ± 0.015	0.021 ± 0.001	0.010 ± 0.011	0.025 ± 0.002	0.028 ± 0.006
Medium	0.007 ± 0.001	0.008 ± 0.002	0.011 ± 0.000	0.009 ± 0.002	0.011 ± 0.001	0.009 ± 0.001
Moderate	0.022 ± 0.002	0.019 ± 0.008	0.009 ± 0.001	0.005 ± 0.006	0.012 ± 0.002	0.013 ± 0.004
Low	0.010 ± 0.000	0.009 ± 0.002	0.007 ± 0.000	0.006 ± 0.002	0.007 ± 0.000	0.008 ± 0.001
Average	0.012 ± 0.001	0.011 ± 0.005	0.007 ± 0.000	0.003 ± 0.004	0.009 ± 0.001	0.015 ± 0.003 0.014 ± 0.001
Nitrification rate (mol/m^2/d)						
High	0.012 ± 0.001	0.011 ± 0.005	0.007 ± 0.000	0.003 ± 0.004	0.009 ± 0.001	0.008 ± 0.002
Medium	0.025 ± 0.007	0.025 ± 0.011	0.010 ± 0.001	0.005 ± 0.006	0.010 ± 0.001	0.015 ± 0.005
Moderate	0.007 ± 0.001	0.006 ± 0.003	0.003 ± 0.000	0.002 ± 0.002	0.004 ± 0.000	0.004 ± 0.001
Low	0.008 ± 0.001	0.007 ± 0.004	0.004 ± 0.000	0.002 ± 0.002	0.004 ± 0.000	0.005 ± 0.001
Average	0.013 ± 0.002	0.012 ± 0.006	0.006 ± 0.001	0.003 ± 0.003	0.007 ± 0.001	0.008 ± 0.003 0.000 ± 0.000

Note. Values are shown as means ± standard deviations for late times (day 365 to day 730) in the simulation. Averages are shown across the sediment (blue, row averages) and water table classes (brown, column averages). The total average for all cases is shown in the bottom right corner for simulations that include biomass growth feedback (green) and do not include biomass growth feedback (red). AR = aerobic respiration; DN = denitrification; and NI = nitrification.

both AR and DN reaction rates decline in the highly losing water table cases (Dry and Atmospheric river). Interestingly, while microbial biomass growth tended to limit *average* reaction rates for DN (With Bio Feedback = 0.046, Without Bio Feedback = 0.084 mol/m^2/d), NI is an example where allowing the biomass feedback led to increased rates (0 mol/m^2/d without the biomass feedback and 0.02 mol/m^2/d with the biomass feedback).

4. Discussion

4.1. Bioclogging-Driven Feedback on Aerobic Respiration and Denitrification

Our results reveal that microbial occupation of sediment pore spaces provides important physical and chemical controls in driving and limiting AR and DN. Physically, biomass provides a unique constraint by limiting transport of substrates, which then introduces a dynamic self-limiting feedback on reaction rates. As such, different reactions can be favored at a single point in time due to variations in substrate delivery from infiltration fluctuations or from biomass-controlled porosity and conductivity changes. An example of this is the biomass control on NI rates, which rely on the presence of O_2 to proceed. NI rates are not initially large enough to provide competition to AR rates. As soon as AR rates decrease, even slightly, from biomass growth, O_2 becomes available for NI to proceed and provides supplementary substrate for DN. Assessment of transient biomass community structure and microbial functional groups will be an important component of future work.

Sediment of the High end-member classification (K^+ Φ^+) representing gravelly riverbeds was found to support the largest microbial growth and initial reaction rates. Sediments of the Medium end-member (K^+ Φ^-), however, were susceptible to early clogging (see supporting information for additional results) that limited substrate delivery providing an important example of the role that initial sediment conditions may have on fate of DOC. In general, coarser sediments provide the greatest potential for turnover without major clogging feedback and remain poised for continual nutrient fluxes. Finer sediments, however, are prone to nutrient and flow inhibition from greater bio-occupation of pore spaces that sufficiently limit respiration rates. In the context of gravelly riverbeds where conflicting and confounding rates of DN have been discussed (B. N. Harvey et al., 2011; Lansdown et al., 2012), this behavior indicates that the direct feedback between sediment structure and microbial growth is a key factor in understanding respiration and DN rates from these settings. Measurement of respiration rates must then be conducted in the context of flow and sediment conditions to fully unravel the evolving and confounding nature of DN in gravelly riverbeds.

We found that inclusion of microbial growth in our numerical modeling framework was necessary to capture the development of the aerobic/anaerobic microzone below the sediment water interface that facilitates the growth of both types of microbes at the same place but at different times. Previous reports of aerobic/anaerobic microzone development have been reported in field settings and suggest that physical heterogeneities in sediment structure can offer an explanation for this development (Briggs et al., 2015). Our results show that microbial growth feedback on fluctuating redox conditions can offer an additional, physical explanation for the development of these microzones through the frequent switch between aerobic and anaerobic conditions.

4.2. Impacts of Losing and Gaining Rivers

Our results show that highly losing rivers (Dry cases) that allow connected and disconnected conditions to occur have larger total infiltration fluxes and overall greater CO_2 and N_2 subsurface production than more gaining rivers. Losing conditions greatly enhanced total C and N transformations and represent significant potential for subsurface C and N sinks. In general, while Fluctuating and Wet conditions greatly limit total C and N transformations, they represent the only significant pathway for biogenic gas release because of temporary gaining conditions. Contrary to losing systems, transitional losing→gaining cases (Average, Fluctuating, and Wet cases) that allow bidirectional flow paths can switch reaction rates on and off because of the delivery versus nondelivery of nutrients from river water. Another pathway for biogenic gas release in natural systems is gas phase advective transport. While our numerical model includes dissolved gas advection/diffusion and gas phase diffusion that allows for gas concentration gradients to provide an exit pathway, our model does not include gas phase advection, which could occur when the water table, for example, physically displaces a gas continuum. Given the possibility of this type of exit pathway, we may

overestimate gas storage and underestimate gas release in highly losing systems and we recommend that future numerical models explicitly account for this physical mechanism.

Our results suggest that hyporheic zone respiration behavior is fundamentally linked to losing versus losing→gaining conditions that shift the balance between uninhibited flow paths that allow fast substrate delivery sustaining biomass growth versus biomass feedback that limit and block those very flow paths. Whether or not a particular system better supports DN reactions over AR reactions is then *conditioned strongly* on flow directions that deliver DOC- and NO_3^--rich water from the surface or nutrient-poor groundwater and how those sediment K_c and Φ characteristics have evolved over time. When water table fluctuations allow a switch in the direction of flow, this halts biomass growth and respiration and allows lysis to begin thereby limiting additional transport rate reductions in favor of larger future reaction rates. Our results suggest that hyporheic zones are not static systems that only support one reaction more than another. Rather, they behave in response to the initial physical conditions set by the river hydrology at the beginning of the summer growing season and show a dynamic range of hyporheic evolutions based on physical feedback and hydrological perturbations providing sufficient conditions for storage or release.

4.3. Fate of DOC

Our results suggest that flow direction, flow magnitude, and sediment characteristics are a strong control on the fate of C and N between subsurface storage as biomass and release to the river as biogenic gas. In general, during losing conditions, between 90 and 100% of all incoming DOC ends up as indefinite storage in the hyporheic zone. During wet conditions, the subsurface stores only 20–40% of incoming DOC. While sediment type may control the proportioning of C to biomass or gases, it is clear that high K_c sediments are the most impactful for large quantities of DOC transformations, with upward of 2–3 times the total amount of DOC processed by the hyporheic zone. In losing rivers with coarse gravelly riverbeds, the hyporheic zone may provide a significant service for total C and N storage and transformation; however, this may be temporary where gaining conditions could quickly reverse net storage due to rare but impactful events such as atmospheric rivers or long wet periods. Since many different field behaviors have been reported for hyporheic zones containing a wide variety of sediment types, we suggest that future studies carefully quantify sediment grain size distributions and water levels near rivers to accurately describe and contextualize reach scale changes in river DOC, DO, NH_4, and NO_3^-.

4.4. Microbially Controlled Evolution of Reaction Rates

Allowing bioclogging to occur within the numerical framework revealed a significant hyporheic biological control on AR and DN rates, typically reducing rates by 30–50% (average of all cases in Tables 2 and 3). If the microbial feedback is neglected in numerical models, respiration and transport rates would never evolve with the physical conditions of the sediment (i.e., Aubeneau et al., 2016), and respiration would continue over time without any physical inhibition. This evolution can be conceptualized using the Damköhler number (*Da*) which is the ratio of the reaction time scale to the transport time scale (time to react to completion/transport time). Smaller reaction rates would increase the reaction time scale (0.1 s^{-1} = 10 s to react to completion, and 0.01 s^{-1} = 100 s to react to completion). In gravelly sediments where conditions are reaction limited (initial *Da* number $>$ 1, reaction time scale $>$ transport time scale), our results support the idea that microbial growth may increase transport times (biomass limitations on K_c) and reduce reaction rates (limited substrate delivery) and allow the *Da* number to evolve toward 1 which is the most efficient state. Indeed, the "optimal" state of hyporheic zones as an integrator for terrestrial processes is an emerging area of research, and we suggest that the role of microbes is one to be highly considered in future numerical model development and field studies. What emerges from the early and late behavior of reaction rates is a useful classification of sediments based on the pulsing of reaction-limited and transport-limited conditions over time and is conceptualized in Figure 8.

4.5. The Role of Hyporheic Zones for River Net Ecosystem Productivity

A conceptual model for the role of hyporheic zones within dry climates is shown in Figure 9 and can be described as follows. In highly losing rivers, such as those found in dry or semiarid climates, different sediment grain size distributions and variability in DOC sources and concentration to subsurface microbes are associated with differences in river flow characteristics during the preceding winter wet season. The fate of

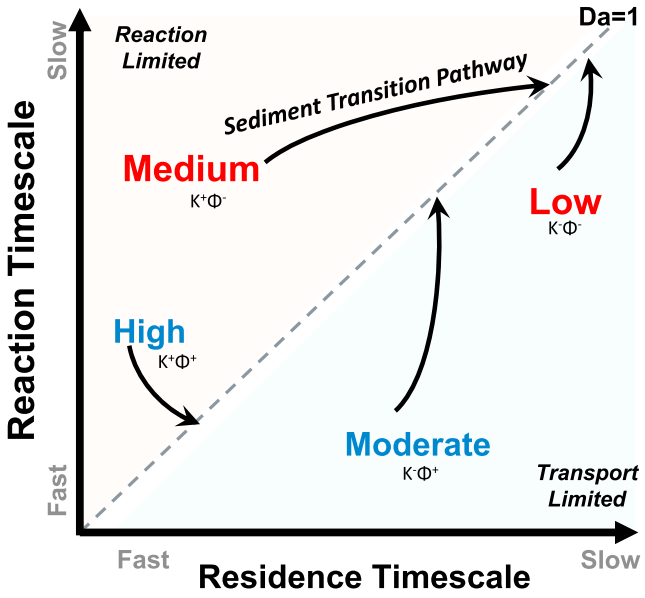

Figure 8. Conceptual model of the evolving Damköhler number (*Da*) for each sediment classification.

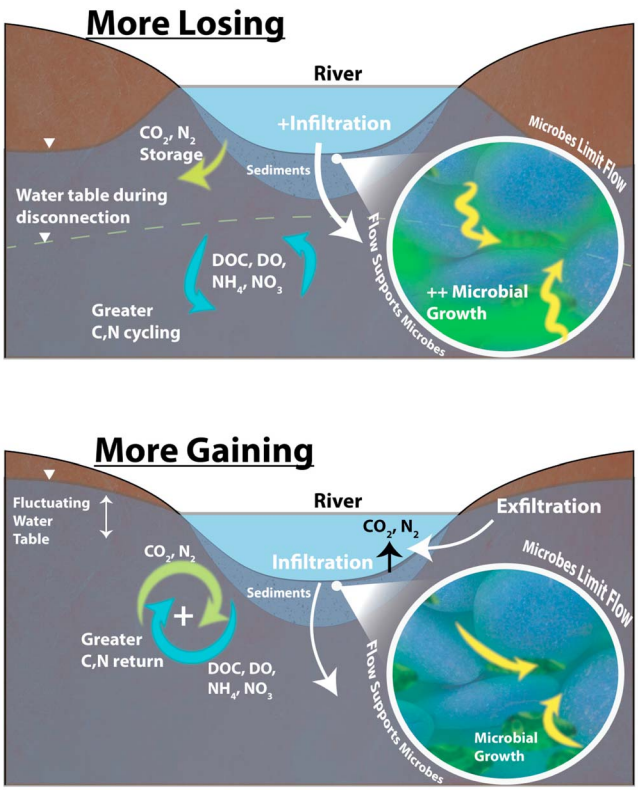

Figure 9. Conceptual model of the river-aquifer interactions that shape biomass growth and reactions within sediments. Reaction rates and transport pathways change over time as sediment microbes grow because of reductions in porosity, conductivity, and reaction rates as flow is inhibited.

DOC between subsurface microbial biomass and biogenic gas release then relies on year-to-year variation due to changes in the characteristics of bed sediments present at the beginning of the growing season and overarching hydrological conditions that can provide an export pathway. Dry climate rivers provide the largest potential for C and N subsurface storage and may contribute little to the hyporheic heterotrophic component in river models of NEP (Butman et al., 2016). Future models of river NEP will need to include the transient conditions and contributions from the hyporheic zone.

At small scales, our results can potentially explain the seemingly paradoxical conditions of complete O_2 removal and DN in gravelly rivers whose fast residence times often confound our understanding of these efficient conditions (Dodds et al., 1996; Findlay, 1995; B. N. Harvey et al., 2011; Lansdown et al., 2012; Vieweg et al., 2016). We suggest that allowing the effects of microbial growth through inclusion of transient parameters in subsurface models can also potentially explain the cumulative controlling effects on reaction rates and residence time distributions of different rivers and may help explain why some transport-limited sediments become reaction limited over time (J. W. Harvey et al., 2013). Accounting for top-down controls of ecology, sediments, dominant flow direction, DOC source and lability, and microbial feedback on infiltration rates and sediment parameters may help resolve this discrepancy.

At larger scales, it is estimated that a particle of water will enter the hyporheic zone numerous times before it reaches a coastal system, thus providing multiple opportunities for river substrates to sustain microbial work through the production of CO_2, N_2 and subsurface storage of C as biomass (Flipo et al., 2014; Gomez-Velez et al., 2015; J. W. Harvey et al., 2013). These physically small zones sustain high biogeochemical gradients and perform their reactions over centimeter scales yet contribute greatly as a major CO_2 source in wet-climate rivers. In dry climates like Mediterranean regions, however, the role of this zone is to store C and N in diverse microbial populations as biomass and dissolved gases rather than release this to the river. Based on this understanding, whether or not the river and hyporheic zone behave as store or source of CO_2 can then be scaled up and classified based on the probability of regional losing or gaining conditions at various locations along a catchment corridor and the sum of those conditions within the dominant climatic regime. Upscaling these results to catchments across different hydrological and climatic conditions is a necessary next step to better account for the role of rivers and hyporheic zones at larger scales, especially given multiscale aspects of river aquifer interactions (Flipo et al., 2014; Pinay et al., 2015). The relative role of these zones is still an area of large research interest and potential, especially in areas where human-based modifications largely overconstrain climatic controls.

4.6. Assumptions and Implications

In our study, we included many major assumptions for the modeling framework: homogeneous sediment structure, 1-D flow, lack of other microbial functional groups (i.e., nitrifiers, sulfate reducers, methanogens, etc.), no groundwater contamination, and loss of gas phase by advection, all of which have implications for model results. In real

riverbed systems, sediment geomorphic structures and heterogeneity within uniform sediment types can induce major preferential flow paths or bottlenecks where the smallest grain size determines the overall flow conditions. Hyporheic flow may be limited in these cases, and our model results representing clean well-sorted gravels may overestimate respiration rates for hyporheic systems. Our assumption of 1-D flow which does not allow more frequent bidirectional exchanges may directly underestimate hyporheic respiration for both losing and gaining systems. Our work included two microbial functional groups as biomass term that allowed C to be mineralized and stored. Inclusion of additional microbial groups that fix CO_2 may reveal that our estimates for storage are greatly underestimated, even for gaining systems.

5. Conclusions

The role of subsurface heterotrophic respiration in total C and N budgets within rivers is highly uncertain. This study mechanistically simulated and assessed the factors controlling heterotrophic growth and resulting hyporheic contributions. We conducted a numerical investigation to study the interactions, feedback, and dependence of bioclogging, and C and N cycling across different sediment and hydrological conditions. This work provides major insights into how coupled biological and physical processes at riverbeds influence two critical ecosystem services: (1) aerobic respiration and DN in the subsurface and (2) hyporheic contributions to NEP in rivers. In general, carbon storage in biomass and CO_2 in the subsurface is not only a function of the initial sediment characteristics that favor biomass growth and C production but also dependent on groundwater-surface water interactions that control whether a perturbation can effectively export that storage to the river. Figure 9 provides a conceptual summary of the role of losing versus gaining rivers on N and C transformations that illuminates complex sediment characteristics and biomass feedback that can change sediment Φ, K_c, and infiltration over time. Our overarching results indicate that hydrological perturbations play a larger role and have a larger control on river C, N transformations, storage, and exports than previously thought. The results also challenge previous assumptions that hyporheic zones largely serve only as sources (rather than also sinks) of biogenic CO_2.

Our numerical results provide the basis for a number of hypotheses that can be tested in future experimental field, laboratory, or numerical research across a range of water table and sediment conditions. Potential avenues of future research include rivers near aquifers with nitrate contamination, riverbeds with significant sediment heterogeneity, microbial controls on gravel bed DN, and controls of changing microbial functional groups in hyporheic and groundwater systems. We suggest that future studies carefully consider the choice of initial sediment parameters and boundary conditions as well as how to represent the feedback of microbial growth in numerical models to accurately describe field-based observations of aerobic respiration rates, seepage, DN potential, and evolution of reaction rates and transport rates over time.

Acknowledgments
This research was supported by the Sonoma County Water Agency (SCWA), the U.S. Department of Energy, Office of Science, Office of Biological and Environmental Research under award DE-AC02-05CH11231 as well as the associated Student Research Fellowship Program and the UFZ-Helmholtz Centre for Environmental Research, Leipzig, Germany. We thank Sally Thompson for the helpful discussions about the significance of the results. We thank Marcus Trotta, Donald Seymour, John Mendoza, and Jay Jasperse of SCWA for their useful suggestions. We also acknowledge the helpful comments and suggestions from three anonymous reviewers that significantly improved the message and readability of our paper. Supplementary appendices, data, and R code can be found in the supporting information of this article.

References

Aalto, R., Maurice-Bourgoin, L., Dunne, T., Montgomery, D. R., Nittrouer, C. A., & Guyot, J.-L. (2003). Episodic sediment accumulation on Amazonian flood plains influenced by El Niño/Southern Oscillation. *Nature*, *425*(6957), 493–497. https://doi.org/10.1038/nature02002

Acuña, V., Giorgi, A., Muñoz, I., Uehlinger, U., & Sabater, S. (2004). Flow extremes and benthic organic matter shape the metabolism of a headwater Mediterranean stream. *Freshwater Biology*, *49*(7), 960–971. https://doi.org/10.1111/j.1365-2427.2004.01239.x

Admiraal, W., & Botermans, Y. H. (1989). Comparison of nitrification rates in three branches of the lower river Rhine. *Biogeochemistry*, *8*(2). https://doi.org/10.1007/BF00001317

Aissa-Grouz, N., Garnier, J., Billen, G., Mercier, B., & Martinez, A. (2015). The response of river nitrification to changes in wastewater treatment (The case of the lower Seine River downstream from Paris). *Annales de Limnologie - International Journal of Limnology*, *51*(4), 351–364. https://doi.org/10.1051/limn/2015031

Andrews, E. D., & Antweiler, R. C. (2012). Sediment fluxes from California coastal rivers: The influences of climate, geology, and topography. *The Journal of Geology*, *120*(4), 349–366. https://doi.org/10.1086/665733

Aqtesolv (2016). Hydraulic properties: Aquifer testing 101. Retrieved from http://www.aqtesolv.com/aquifer-tests/aquifer_properties.htm, (Accessed date November 20, 2016).

Aubeneau, A. F., Hanrahan, B., Bolster, D., & Tank, J. (2016). Biofilm growth in gravel bed streams controls solute residence time distributions. *Journal of Geophysical Research: Biogeosciences*, *121*, 1840–1850. https://doi.org/10.1002/2016JG003333

Azizian, M., Boano, F., Cook, P. L. M., Detwiler, R. L., Rippy, M. A., & Grant, S. B. (2017). Ambient groundwater flow diminishes nitrate processing in the hyporheic zone of streams. *Water Resources Research*, *53*, 3941–3967. https://doi.org/10.1002/2016WR020048

Baratelli, F., Flipo, N., & Moatar, F. (2016). Estimation of stream-aquifer exchanges at regional scale using a distributed model: Sensitivity to in-stream water level fluctuations, riverbed elevation and roughness. *Journal of Hydrology*, *542*, 686–703. https://doi.org/10.1016/j.jhydrol.2016.09.041

Battin, T. J., Besemer, K., Bengtsson, M. M., Romani, A. M., & Packmann, A. I. (2016). The ecology and biogeochemistry of stream biofilms. *Nature Reviews Microbiology*, *14*(4), 251–263. https://doi.org/10.1038/nrmicro.2016.15

Battin, T. J., Kaplan, L. A., Findlay, S., Hopkinson, C. S., Marti, E., Packman, A. I., et al. (2008). Biophysical controls on organic carbon fluxes in fluvial networks. *Nature Geoscience*, *1*(2), 95–100. https://doi.org/10.1038/ngeo101

Beard, D. C., & Weyl, P. K. (1973). Influence of texture on porosity and permeability of unconsolidated sand. *AAPG Bulletin*, *57*(2), 349–369.
Boadu, F. K. (2000). Hydraulic conductivity of soils from grain-size distribution: New models. *Journal of Geotechnical and Geoenvironmental Engineering*, *126*(8), 739–746. https://doi.org/10.1061/(ASCE)1090-0241(2000)126:8(739)
Bonada, N., & Resh, V. H. (2013). Mediterranean-climate streams and rivers: Geographically separated but ecologically comparable freshwater systems. *Hydrobiologia*, *719*(1), 1–29. https://doi.org/10.1007/s10750-013-1634-2
Briggs, M. A., Day-Lewis, F. D., Zarnetske, J. P., & Harvey, J. W. (2015). A physical explanation for the development of redox microzones in hyporheic flow. *Geophysical Research Letters*, *42*, 4402–4410. https://doi.org/10.1002/2015GL064200
Brovelli, A., Malaguerra, F., & Barry, D. A. (2009). Bioclogging in porous media: Model development and sensitivity to initial conditions. *Environmental Modelling & Software*, *24*(5), 611–626. https://doi.org/10.1016/j.envsoft.2008.10.001
Brunner, P., Cook, P. G., & Simmons, C. T. (2009). Hydrogeologic controls on disconnection between surface water and groundwater. *Water Resources Research*, *45*, W01422. https://doi.org/10.1029/2008WR006953
Brunner, P., Simmons, C. T., & Cook, P. G. (2009). Spatial and temporal aspects of the transition from connection to disconnection between rivers, lakes and groundwater. *Journal of Hydrology*, *376*(1–2), 159–169. https://doi.org/10.1016/j.jhydrol.2009.07.023
Butman, D., Stackpoole, S., Stets, E., McDonald, C. P., Clow, D. W., & Striegl, R. G. (2016). Aquatic carbon cycling in the conterminous United States and implications for terrestrial carbon accounting. *Proceedings of the National Academy of Sciences*, *113*(1), 58–63. https://doi.org/10.1073/pnas.1512651112
Canfield, D., Jørgensen, B., Fossing, H., Glud, R., Gundersen, J., Ramsing, N., et al. (1993). Pathways of organic carbon oxidation in three continental margin sediments. *Marine Geology*, *113*(1–2), 27–40. https://doi.org/10.1016/0025-3227(93)90147-N
Caruso, A., Boano, F., Ridolfi, L., Chopp, D. L., & Packman, A. (2017). Biofilm-induced bioclogging produces sharp interfaces in hyporheic flow, redox conditions, and microbial community structure. *Geophysical Research Letters*, *44*, 4917–4925. https://doi.org/10.1002/2017GL073651
Casas-Ruiz, J. P., Tittel, J., von Schiller, D., Catalán, N., Obrador, B., Gómez-Gener, L., et al. (2016). Drought-induced discontinuities in the source and degradation of dissolved organic matter in a Mediterranean river. *Biogeochemistry*, *127*(1), 125–139. https://doi.org/10.1007/s10533-015-0173-5
Cayan, D. R., Redmond, K. T., & Riddle, L. G. (1999). ENSO and hydrologic extremes in the western United States. *Journal of Climate*, *12*(9), 2881–2893. https://doi.org/10.1175/1520-0442(1999)012%3C2881:EAHEIT%3E2.0.CO;2
Chen, W., Huang, C., Chang, M., Chang, P., & Lu, H. (2013). The impact of floods on infiltration rates in a disconnected stream. *Water Resources Research*, *49*, 7887–7899. https://doi.org/10.1002/2013WR013762
Chen, X., Burbach, M., & Cheng, C. (2008). Electrical and hydraulic vertical variability in channel sediments and its effects on streamflow depletion due to groundwater extraction. *Journal of Hydrology*, *352*(3–4), 250–266. https://doi.org/10.1016/j.jhydrol.2008.01.004
Crosbie, R. S., Taylor, A. R., Davis, A. C., Lamontagne, S., & Munday, T. (2014). Evaluation of infiltration from losing-disconnected rivers using a geophysical characterisation of the riverbed and a simplified infiltration model. *Journal of Hydrology*, *508*, 102–113. https://doi.org/10.1016/j.jhydrol.2013.07.045
Cuthbert, M. O., Mackay, R., Durand, V., Aller, M.-F., Greswell, R. B., & Rivett, M. O. (2010). Impacts of river bed gas on the hydraulic and thermal dynamics of the hyporheic zone. *Advances in Water Resources*, *33*(11), 1347–1358. https://doi.org/10.1016/j.advwatres.2010.09.014
Deitch, M., Sapundjieff, M., & Feirer, S. (2017). Characterizing precipitation variability and trends in the world's Mediterranean-climate areas. *Watermark*, *9*(12), 259. https://doi.org/10.3390/w9040259
Dettinger, M. D., Ralph, F. M., Das, T., Neiman, P. J., & Cayan, D. R. (2011). Atmospheric rivers, floods and the water resources of California. *Watermark*, *3*(4), 445–478. https://doi.org/10.3390/w3020445
Dodds, W. K., Randel, C. A., & Edler, C. C. (1996). Microcosms for aquifer research: Application to colonization of various sized particles by ground-water microorganisms. *Ground Water*, *34*(4), 756–759. https://doi.org/10.1111/j.1745-6584.1996.tb02065.x
Dupin, H. J., Kitanidis, P. K., & McCarty, P. L. (2001). Pore-scale modeling of biological clogging due to aggregate expansion: A material mechanics approach. *Water Resources Research*, *37*(12), 2965–2979. https://doi.org/10.1029/2001WR000306
ElBishlawi, H., & Jaffe, P. R. (2015). Characterization of dissolved organic matter from a restored urban marsh and its role in the mobilization of trace metals. *Chemosphere*, *127*, 144–151. https://doi.org/10.1016/j.chemosphere.2014.12.080
Escoffier, N., Bensoussan, N., Vilmin, L., Flipo, N., Rocher, V., David, A., et al. (2016). Estimating ecosystem metabolism from continuous multi-sensor measurements in the Seine River. *Environmental Science and Pollution Research*. https://doi.org/10.1007/s11356-016-7096-0
Ezeuko, C. C., Sen, A., Grigoryan, A., & Gates, I. D. (2011). Pore-network modeling of biofilm evolution in porous media. *Biotechnology and Bioengineering*, *108*(10), 2413–2423. https://doi.org/10.1002/bit.23183
Findlay, S. (1995). Importance of surface-subsurface exchange in stream ecosystems: The hyporheic zone. *Limnology and Oceanography*, *40*(1), 159–164. https://doi.org/10.4319/lo.1995.40.1.0159
Fleckenstein, J. H., Niswonger, R. G., & Fogg, G. E. (2006). River-aquifer interactions, geologic heterogeneity, and low-flow management. *Ground Water*, *44*(6 Understanding), 837–852. https://doi.org/10.1111/j.1745-6584.2006.00190.x
Flipo, N., Even, S., Poulin, M., Tusseau-Vuillemin, M.-H., Ameziane, T., & Dauta, A. (2004). Biogeochemical modelling at the river scale: Plankton and periphyton dynamics. *Ecological Modelling*, *176*(3–4), 333–347. https://doi.org/10.1016/j.ecolmodel.2004.01.012
Flipo, N., Jeannée, N., Poulin, M., Even, S., & Ledoux, E. (2007). Assessment of nitrate pollution in the Grand Morin aquifers (France): Combined use of geostatistics and physically based modeling. *Environmental Pollution*, *146*(1), 241–256. https://doi.org/10.1016/j.envpol.2006.03.056
Flipo, N., Mouhri, A., Labarthe, B., Biancamaria, S., Rivière, A., & Weill, P. (2014). Continental hydrosystem modelling: The concept of nested stream-aquifer interfaces. *Hydrology and Earth System Sciences*, *18*(8), 3121–3149. https://doi.org/10.5194/hess-18-3121-2014
Flipo, N., Rabouille, C., Poulin, M., Even, S., Tusseau-Vuillemin, M.-H., & Lalande, M. (2007). Primary production in headwater streams of the Seine basin: The Grand Morin river case study. *Science of the Total Environment*, *375*(1–3), 98–109. https://doi.org/10.1016/j.scitotenv.2006.12.015
Fox, A., Laube, G., Schmidt, C., Fleckenstein, J. H., & Arnon, S. (2016). The effect of losing and gaining flow conditions on hyporheic exchange in heterogeneous streambeds. *Water Resources Research*, *52*, 7460–7477. https://doi.org/10.1002/2016WR018677
Garcia-ruiz, R., Pattinson, S. N., & Whitton, B. A. (1998). Denitrification in river sediments: Relationship between process rate and properties of water and sediment. *Freshwater Biology*, *39*(3), 467–476. https://doi.org/10.1046/j.1365-2427.1998.00295.x
Geotechdata (2008). Soil permeability—Geotechdata.Info. Retrieved from http://www.geotechdata.info/parameter/permeability.html, (Accessed date November 20, 2016).
Gomez-Velez, J. D., Harvey, J. W., Cardenas, M. B., & Kiel, B. (2015). Denitrification in the Mississippi River network controlled by flow through river bedforms. *Nature Geoscience*, *8*(12), 941–945. https://doi.org/10.1038/ngeo2567

Gray, A. B., Pasternack, G. B., Watson, E. B., Warrick, J. A., & Goñi, M. A. (2015a). Effects of antecedent hydrologic conditions, time dependence, and climate cycles on the suspended sediment load of the Salinas River, California. *Journal of Hydrology*, *525*, 632–649. https://doi.org/10.1016/j.jhydrol.2015.04.025

Gray, A. B., Pasternack, G. B., Watson, E. B., Warrick, J. A., & Goñi, M. A. (2015b). The effect of El Niño Southern Oscillation cycles on the decadal scale suspended sediment behavior of a coastal dry-summer subtropical catchment. *Earth Surface Processes and Landforms*, *40*(2), 272–284. https://doi.org/10.1002/esp.3627

Hall, R. O., Tank, J. L., Baker, M. A., Rosi-Marshall, E. J., & Hotchkiss, E. R. (2015). Metabolism, gas exchange, and carbon spiraling in rivers. *Ecosystems*, *19*(1), 73–86. https://doi.org/10.1007/s10021-015-9918-1

Harvey, B. N., Johnson, M. L., Kiernan, J. D., & Green, P. G. (2011). Net dissolved inorganic nitrogen production in hyporheic mesocosms with contrasting sediment size distributions. *Hydrobiologia*, *658*(1), 343–352. https://doi.org/10.1007/s10750-010-0504-4

Harvey, J. W., Böhlke, J. K., Voytek, M. A., Scott, D., & Tobias, C. R. (2013). Hyporheic zone denitrification: Controls on effective reaction depth and contribution to whole-stream mass balance: Scaling hyporheic flow controls on stream denitrification. *Water Resources Research*, *49*, 6298–6316. https://doi.org/10.1002/wrcr.20492

Harvey, J. W., & Gooseff, M. (2015). River corridor science: Hydrologic exchange and ecological consequences from bedforms to basins. *Water Resources Research*, *51*, 6893–6922. https://doi.org/10.1002/2015WR017617

Hatch, C. E., Fisher, A. T., Ruehl, C. R., & Stemler, G. (2010). Spatial and temporal variations in streambed hydraulic conductivity quantified with time-series thermal methods. *Journal of Hydrology*, *389*(3–4), 276–288. https://doi.org/10.1016/j.jhydrol.2010.05.046

Höpfner, M., Milz, M., Buehler, S., Orphal, J., & Stiller, G. (2012). The natural greenhouse effect of atmospheric oxygen (O_2) and nitrogen (N_2). *Geophysical Research Letters*, *39*, L10706. https://doi.org/10.1029/2012GL051409

Hotchkiss, E. R., Hall, R. O. Jr., Sponseller, R. A., Butman, D., Klaminder, J., Laudon, H., et al. (2015). Sources of and processes controlling CO_2 emissions change with the size of streams and rivers. *Nature Geoscience*, *8*(9), 696–699. https://doi.org/10.1038/ngeo2507

Hou, Z., Nelson, W. C., Stegen, J. C., Murray, C. J., Arntzen, E., Crump, A. R., et al. (2017). Geochemical and microbial community attributes in relation to hyporheic zone geological facies. *Scientific Reports*, *7*(1), 12006. https://doi.org/10.1038/s41598-017-12275-w

Inman, D. L., & Jenkins, S. A. (1999). Climate change and the episodicity of sediment flux of small California rivers. *The Journal of Geology*, *107*(3), 251–270. https://doi.org/10.1086/314346

Irvine, D. J., Brunner, P., Franssen, H.-J. H., & Simmons, C. T. (2012). Heterogeneous or homogeneous? Implications of simplifying heterogeneous streambeds in models of losing streams. *Journal of Hydrology*, *424-425*, 16–23. https://doi.org/10.1016/j.jhydrol.2011.11.051

Kalbus, E., Schmidt, C., Molson, J. W., Reinstorf, F., & Schirmer, M. (2009). Influence of aquifer and streambed heterogeneity on the distribution of groundwater discharge. *Hydrology and Earth System Sciences*, *13*(1), 69–77. https://doi.org/10.5194/hess-13-69-2009

Kamann, P. J., Ritzi, R. W., Dominic, D. F., & Conrad, C. M. (2007). Porosity and permeability in sediment mixtures. *Ground Water*, *45*(4), 429–438. https://doi.org/10.1111/j.1745-6584.2007.00313.x

Kaplan, L. A., & Bott, T. L. (1982). Diel fluctuations of DOC generated by algae in a Piedmont stream. *Limnology and Oceanography*, *27*(6), 1091–1100. https://doi.org/10.4319/lo.1982.27.6.1091

Kaplan, L. A., & Bott, T. L. (1989). Diel fluctuations in bacterial activity on streambed substrata during vernal algal blooms: Effects of temperature, water chemistry, and habitat. *Limnology and Oceanography*, *34*(4), 718–733. https://doi.org/10.4319/lo.1989.34.4.0718

Karwan, D. L., & Saiers, J. E. (2012). Hyporheic exchange and streambed filtration of suspended particles. *Water Resources Research*, *48*, W01519. https://doi.org/10.1029/2011WR011173

Kildsgaard, J., & Engesgaard, P. (2001). Numerical analysis of biological clogging in two-dimensional sand box experiments. *Journal of Contaminant Hydrology*, *50*(3–4), 261–285. https://doi.org/10.1016/S0169-7722(01)00109-7

Kolbjørn Jensen, J., Engesgaard, P., Johnsen, A. R., Marti, V., & Nilsson, B. (2017). Hydrological mediated denitrification in groundwater below a seasonal flooded restored riparian zone: Denitrification in groundwater below flooded riparian zone. *Water Resources Research*, *53*, 2074–2094. https://doi.org/10.1002/2016WR019581

Kondrashov, D. (2005). Oscillatory modes of extended Nile River records (A.D. 622–1922). *Geophysical Research Letters*, *32*, L10702. https://doi.org/10.1029/2004GL022156

Lamontagne, S., Taylor, A. R., Cook, P. G., Crosbie, R. S., Brownbill, R., Williams, R. M., & Brunner, P. (2013). Field assessment of surface water-groundwater connectivity in a semi-arid river basin (Murray-Darling, Australia). *Hydrological Processes*, *28*(4), 1561–1572. https://doi.org/10.1002/hyp.9691

Lansdown, K., Trimmer, M., Heppell, C. M., Sgouridis, F., Ullah, S., Heathwaite, A. L., et al. (2012). Characterization of the key pathways of dissimilatory nitrate reduction and their response to complex organic substrates in hyporheic sediments. *Limnology and Oceanography*, *57*(2), 387–400. https://doi.org/10.4319/lo.2012.57.2.0387

Larned, S. T., Gooseff, M. N., Packman, A. I., Rugel, K., & Wondzell, S. M. (2015). Groundwater–surface-water interactions: Current research directions. *Freshwater Science*, *34*(1), 92–98. https://doi.org/10.1086/679491

Lavers, D. A., Hannah, D. M., & Bradley, C. (2015). Connecting large-scale atmospheric circulation, river flow and groundwater levels in a chalk catchment in southern England. *Journal of Hydrology*, *523*, 179–189. https://doi.org/10.1016/j.jhydrol.2015.01.060

Leonardson, R. (2010). *Exchange of Fine Sediments With Gravel Riverbeds*. Berkeley: University of California.

Mann, C. J., & Wetzel, R. G. (1995). Dissolved organic carbon and its utilization in a riverine wetland ecosystem. *Biogeochemistry*, *31*(2), 99–120.

Marcarelli, A. M., Huckins, C. J., & Eggert, S. L. (2015). Sand aggradation alters biofilm standing crop and metabolism in a low-gradient Lake Superior tributary. *Journal of Great Lakes Research*, *41*(4), 1052–1059. https://doi.org/10.1016/j.jglr.2015.09.004

Marmonier, P., Archambaud, G., Belaidi, N., Bougon, N., Breil, P., Chauvet, E., et al. (2012). The role of organisms in hyporheic processes: Gaps in current knowledge, needs for future research and applications. *Annales de Limnologie - International Journal of Limnology*, *48*(3), 253–266. https://doi.org/10.1051/limn/2012009

Matsunaga, T., Karametaxas, G., von Gunten, H. R., & Lichtner, P. C. (1993). Redox chemistry of iron and manganese minerals in river-recharged aquifers: A model interpretation of a column experiment. *Geochimica et Cosmochimica Acta*, *57*(8), 1691–1704. https://doi.org/10.1016/0016-7037(93)90107-8

Mayer, K. U., Frind, E. O., & Blowes, D. W. (2002). Multicomponent reactive transport modeling in variably saturated porous media using a generalized formulation for kinetically controlled reactions. *Water Resources Research*, *38*(9), 1174. https://doi.org/10.1029/2001WR000862

McCallum, A. M., Andersen, M. S., Giambastiani, B. M. S., Kelly, B. F. J., & Ian Acworth, R. (2013). River–aquifer interactions in a semi-arid environment stressed by groundwater abstraction. *Hydrological Processes*, *27*(7), 1072–1085. https://doi.org/10.1002/hyp.9229

McCallum, J. L., & Shanafield, M. (2016). Residence times of stream-groundwater exchanges due to transient stream stage fluctuations. *Water Resources Research*, *52*, 2059–2073. https://doi.org/10.1002/2015WR017441

Molz, F. J., Widdowson, M. A., & Benefield, L. D. (1986). Simulation of microbial growth dynamics coupled to nutrient and oxygen transport in porous media. *Water Resources Research*, *22*(8), 1207–1216. https://doi.org/10.1029/WR022i008p01207

Murphy, E. M., & Ginn, T. R. (2000). Modeling microbial processes in porous media. *Hydrogeology Journal*, *8*(1), 142–158. https://doi.org/10.1007/s100409900043

Mutiti, S., & Levy, J. (2010). Using temperature modeling to investigate the temporal variability of riverbed hydraulic conductivity during storm events. *Journal of Hydrology*, *388*(3–4), 321–334. https://doi.org/10.1016/j.jhydrol.2010.05.011

Newcomer, M. E., Hubbard, S. S., Fleckenstein, J. H., Maier, U., Schmidt, C., Thullner, M., et al. (2016). Simulating bioclogging effects on dynamic riverbed permeability and infiltration. *Water Resources Research*, *52*, 2883–2900. https://doi.org/10.1002/2015WR018351

Odum, H. T. (1956). Primary production in flowing waters. *Limnology and Oceanography*, *1*(2), 102–117. https://doi.org/10.4319/lo.1956.1.2.0102

Oyarzún, R., Barrera, F., Salazar, P., Maturana, H., Oyarzún, J., Aguirre, E., et al. (2014). Multi-method assessment of connectivity between surface water and shallow groundwater: The case of Limarí River basin, north-central Chile. *Hydrogeology Journal*, *22*(8), 1857–1873. https://doi.org/10.1007/s10040-014-1170-9

Petticrew, E. L., Krein, A., & Walling, D. E. (2007). Evaluating fine sediment mobilization and storage in a gravel-bed river using controlled reservoir releases. *Hydrological Processes*, *21*(2), 198–210. https://doi.org/10.1002/hyp.6183

Peyrard, D., Delmotte, S., Sauvage, S., Namour, P., Gerino, M., Vervier, P., & Sanchez-Perez, J. M. (2011). Longitudinal transformation of nitrogen and carbon in the hyporheic zone of an N-rich stream: A combined modelling and field study. *Physics and Chemistry of the Earth*, *36*(12), 599–611. https://doi.org/10.1016/j.pce.2011.05.003

Pinay, G., Peiffer, S., De Dreuzy, J.-R., Krause, S., Hannah, D. M., Fleckenstein, J. H., et al. (2015). Upscaling nitrogen removal capacity from local hotspots to low stream orders' drainage basins. *Ecosystems*, *18*(6), 1101–1120. https://doi.org/10.1007/s10021-015-9878-5

Plant, R. E. (2012). *Spatial Data Analysis in Ecology and Agriculture Using R*. Boca Raton: CRC Press. Retrieved from http://www.crcnetbase.com/isbn/9781439819142, https://doi.org/10.1201/b11769

Power, M. E. (1992). Hydrologic and trophic controls of seasonal algal blooms in northern California rivers. *Archiv für Hydrobiologie*, *125*(4), 385–410.

Power, M. E., Lowe, R., Furey, P., Welter, J., Limm, M., Finlay, J., et al. (2009). Algal mats and insect emergence in rivers under Mediterranean climates: Towards photogrammetric surveillance. *Freshwater Biology*, *54*(10), 2101–2115. https://doi.org/10.1111/j.1365-2427.2008.02163.x

Power, M. E., Parker, M. S., & Dietrich, W. E. (2008). Seasonal reassembly of a river food web: Floods, droughts, and impacts of fish. *Ecological Monographs*, *78*(2), 263–282. https://doi.org/10.1890/06-0902.1

Pryet, A., Labarthe, B., Saleh, F., Akopian, M., & Flipo, N. (2015). Reporting of stream-aquifer flow distribution at the regional scale with a distributed process-based model. *Water Resources Management*, *29*(1), 139–159. https://doi.org/10.1007/s11269-014-0832-7

Raimonet, M., Vilmin, L., Flipo, N., Rocher, V., & Laverman, A. M. (2015). Modelling the fate of nitrite in an urbanized river using experimentally obtained nitrifier growth parameters. *Water Research*, *73*, 373–387. https://doi.org/10.1016/j.watres.2015.01.026

Ranalli, A. J., & Macalady, D. L. (2010). The importance of the riparian zone and in-stream processes in nitrate attenuation in undisturbed and agricultural watersheds—A review of the scientific literature. *Journal of Hydrology*, *389*(3–4), 406–415. https://doi.org/10.1016/j.jhydrol.2010.05.045

Ritz, S., Dähnke, K., & Fischer, H. (2018). Open-channel measurement of denitrification in a large lowland river. *Aquatic Sciences*, *80*(1). https://doi.org/10.1007/s00027-017-0560-1

Rivett, M. O., Buss, S. R., Morgan, P., Smith, J. W. N., & Bemment, C. D. (2008). Nitrate attenuation in groundwater: A review of biogeochemical controlling processes. *Water Research*, *42*(16), 4215–4232. https://doi.org/10.1016/j.watres.2008.07.020

Rivière, A., Gonçalvès, J., Jost, A., & Font, M. (2014). Experimental and numerical assessment of transient stream–aquifer exchange during disconnection. *Journal of Hydrology*, *517*, 574–583. https://doi.org/10.1016/j.jhydrol.2014.05.040

Rockhold, M. L., Yarwood, R. R., Niemet, M. R., Bottomley, P. J., & Selker, J. S. (2005). Experimental observations and numerical modeling of coupled microbial and transport processes in variably saturated sand. *Vadose Zone Journal*, *4*(2), 407. https://doi.org/10.2136/vzj2004.0087

Rode, M., Hartwig, M., Wagenschein, D., Kebede, T., & Borchardt, D. (2015). The importance of hyporheic zone processes on ecological functioning and solute transport of streams and rivers. In L. Chicharo, F. Müller, & N. Fohrer (Eds.), *Ecosystem Services and River Basin Ecohydrology* (pp. 57–82). Dordrecht, Netherlands: Springer. Retrieved from http://link.springer.com/10.1007/978-94-017-9846-4_4

Rosenberry, D. O., Klos, P. Z., & Neal, A. (2012). In situ quantification of spatial and temporal variability of hyporheic exchange in static and mobile gravel-bed rivers. *Hydrological Processes*, *26*(4), 604–612. https://doi.org/10.1002/hyp.8154

Rosenzweig, R., Furman, A., Dosoretz, C., & Shavit, U. (2014). Modeling biofilm dynamics and hydraulic properties in variably saturated soils using a channel network model. *Water Resources Research*, *50*, 5678–5697. https://doi.org/10.1002/2013WR015211

Samsó, R., García, J., Molle, P., & Forquet, N. (2016). Modelling bioclogging in variably saturated porous media and the interactions between surface/subsurface flows: Application to constructed wetlands. *Journal of Environmental Management*, *165*, 271–279. https://doi.org/10.1016/j.jenvman.2015.09.045

Sapriza-Azuri, G., Jódar, J., Navarro, V., Slooten, L. J., Carrera, J., & Gupta, H. V. (2015). Impacts of rainfall spatial variability on hydrogeological response. *Water Resources Research*, *51*, 1300–1314. https://doi.org/10.1002/2014WR016168

Sawyer, A. H., & Cardenas, M. B. (2009). Hyporheic flow and residence time distributions in heterogeneous cross-bedded sediment. *Water Resources Research*, *45*, W08406. https://doi.org/10.1029/2008WR007632

Schälchli, U. (1992). The clogging of coarse gravel river beds by fine sediment. *Hydrobiologia*, *235-236*(1), 189–197. https://doi.org/10.1007/BF00026211

Seitzinger, S., Harrison, J. A., Böhlke, J. K., Bouwman, A. F., Lowrance, R., Peterson, B., et al. (2006). Denitrifcation across landscapes and watersheds: A synthesis. *Ecological Applications*, *16*(6), 2064–2090. https://doi.org/10.1890/1051-0761(2006)016%5B2064,DALAWA%5D2.0.CO;2

Sheibley, R. W., Jackman, A. P., Duff, J. H., & Triska, F. J. (2003). Numerical modeling of coupled nitrification-denitrification in sediment perfusion cores from the hyporheic zone of the Shingobee River, MN. *Advances in Water Resources*, *26*(9), 977–987. https://doi.org/10.1016/S0309-1708(03)00088-5

Shepherd, R. G. (1989). Correlations of permeability and grain size. *Ground Water*, *27*(5), 633–638. https://doi.org/10.1111/j.1745-6584.1989.tb00476.x

Slatt, R. M. (2006). *Stratigraphic Reservoir Characterization for Petroleum Geologists, Geophysicists, and Engineers*. Amsterdam; Oxford: Elsevier. Retrieved from http://site.ebrary.com/id/10155827

Sneider, R. M. (1987). *Practical Petrophysics for Exploration and Development (AAPG Education Department Short Course Notes)*. Houston, TX: AAPG.

Spalding, R. F., & Exner, M. E. (1993). Occurrence of nitrate in groundwater—A review. *Journal of Environmental Quality*, *22*(3), 392. https://doi.org/10.2134/jeq1993.00472425002200030002x

Strauss, E. A., Richardson, W. B., Bartsch, L. A., Cavanaugh, J. C., Bruesewitz, D. A., Imker, H., et al. (2004). Nitrification in the upper Mississippi River: Patterns, controls, and contribution to the NO_3^- budget. *Journal of the North American Benthological Society*, *23*(1), 1–14. https://doi.org/10.1899/0887-3593(2004)023%3C0001:NITUMR%3E2.0.CO;2

Su, G. W., Jasperse, J., Seymour, D., & Constantz, J. (2004). Estimation of hydraulic conductivity in an alluvial system using temperatures. *Ground Water*, *42*(6), 890–901. https://doi.org/10.1111/j.1745-6584.2004.t01-7-.x

Su, G. W., Jasperse, J., Seymour, D., Constantz, J., & Zhou, Q. (2007). Analysis of pumping-induced unsaturated regions beneath a perennial river. *Water Resources Research*, *43*, W08421. https://doi.org/10.1029/2006WR005389

Sudduth, E. B., Perakis, S. S., & Bernhardt, E. S. (2013). Nitrate in watersheds: Straight from soils to streams. *Journal of Geophysical Research: Biogeosciences*, *118*, 291–302. https://doi.org/10.1002/jgrg.20030

Tang, Q., Kurtz, W., Brunner, P., Vereecken, H., & Hendricks Franssen, H.-J. (2015). Characterisation of river–aquifer exchange fluxes: The role of spatial patterns of riverbed hydraulic conductivities. *Journal of Hydrology*, *531*, 111–123. https://doi.org/10.1016/j.jhydrol.2015.08.019

Taylor, A. R., Lamontagne, S., & Crosbie, R. S. (2013). Measurements of riverbed hydraulic conductivity in a semi-arid lowland river system (Murray–Darling Basin, Australia). *Soil Research*, *51*(5), 363. https://doi.org/10.1071/SR13090

Thullner, M. (2010). Comparison of bioclogging effects in saturated porous media within one- and two-dimensional flow systems. *Ecological Engineering*, *36*(2), 176–196. https://doi.org/10.1016/j.ecoleng.2008.12.037

Thullner, M., Mauclaire, L., Schroth, M. H., Kinzelbach, W., & Zeyer, J. (2002). Interaction between water flow and spatial distribution of microbial growth in a two-dimensional flow field in saturated porous media. *Journal of Contaminant Hydrology*, *58*(3–4), 169–189. https://doi.org/10.1016/S0169-7722(02)00033-5

Thullner, M., Regnier, P., & Van Cappellen, P. (2007). Modeling microbially induced carbon degradation in redox-stratified subsurface environments: Concepts and open questions. *Geomicrobiology Journal*, *24*(3–4), 139–155. https://doi.org/10.1080/01490450701459275

Thullner, M., Schroth, M. H., Zeyer, J., & Kinzelbach, W. (2004). Modeling of a microbial growth experiment with bioclogging in a two-dimensional saturated porous media flow field. *Journal of Contaminant Hydrology*, *70*(1–2), 37–62. https://doi.org/10.1016/j.jconhyd.2003.08.008

Thullner, M., Van Cappellen, P., & Regnier, P. (2005). Modeling the impact of microbial activity on redox dynamics in porous media. *Geochimica et Cosmochimica Acta*, *69*(21), 5005–5019. https://doi.org/10.1016/j.gca.2005.04.026

Thullner, M., Zeyer, J., & Kinzelbach, W. (2002). Influence of microbial growth on hydraulic properties of pore networks. *Transport in Porous Media*, *49*(1), 99–122. https://doi.org/10.1023/A:1016030112089

Tonina, D., de Barros, F. P. J., Marzadri, A., & Bellin, A. (2016). Does streambed heterogeneity matter for hyporheic residence time distribution in sand-bedded streams? *Advances in Water Resources*, *96*, 120–126. https://doi.org/10.1016/j.advwatres.2016.07.009

Trauth, N., & Fleckenstein, J. H. (2017). Single discharge events increase reactive efficiency of the hyporheic zone. *Water Resources Research*, *53*, 779–798. https://doi.org/10.1002/2016WR019488

Trauth, N., Schmidt, C., Vieweg, M., Maier, U., & Fleckenstein, J. H. (2014). Hyporheic transport and biogeochemical reactions in pool-riffle systems under varying ambient groundwater flow conditions. *Journal of Geophysical Research: Biogeosciences*, *119*, 910–928. https://doi.org/10.1002/2013JG002586

Trauth, N., Schmidt, C., Vieweg, M., Oswald, S. E., & Fleckenstein, J. H. (2015). Hydraulic controls of in-stream gravel bar hyporheic exchange and reactions. *Water Resources Research*, *51*, 2243–2263. https://doi.org/10.1002/2014WR015857

Treese, S., Meixner, T., & Hogan, J. F. (2009). Clogging of an effluent dominated semiarid river: A conceptual model of stream-aquifer interactions. *JAWRA Journal of the American Water Resources Association*, *45*(4), 1047–1062. https://doi.org/10.1111/j.1752-1688.2009.00346.x

Ulrich, C., Hubbard, S., Florsheim, J., Rosenberry, D. O., Borglin, S., Trotta, M., & Seymour, D. (2015). Riverbed clogging associated with a California riverbank filtration system: An assessment of mechanisms and monitoring approaches. *Journal of Hydrology*, *529*(3), 1740–1753. https://doi.org/10.1016/j.jhydrol.2015.08.012

Vico, G., Thompson, S. E., Manzoni, S., Molini, A., Albertson, J. D., Almeida-Cortez, J. S., et al. (2015). Climatic, ecophysiological, and phenological controls on plant ecohydrological strategies in seasonally dry ecosystems. *Ecohydrology*, *8*(4), 660–681. https://doi.org/10.1002/eco.1533

Vieweg, M., Kurz, M. J., Trauth, N., Fleckenstein, J. H., Musolff, A., & Schmidt, C. (2016). Estimating time-variable aerobic respiration in the streambed by combining electrical conductivity and dissolved oxygen time series. *Journal of Geophysical Research: Biogeosciences*, *121*, 2199–2215. https://doi.org/10.1002/2016JG003345

Vilmin, L., Flipo, N., de Fouquet, C., & Poulin, M. (2015). Pluri-annual sediment budget in a navigated river system: The Seine River (France). *Science of the Total Environment*, *502*, 48–59. https://doi.org/10.1016/j.scitotenv.2014.08.110

Vilmin, L., Flipo, N., Escoffier, N., & Groleau, A. (2016). Estimation of the water quality of a large urbanized river as defined by the European WFD: What is the optimal sampling frequency? *Environmental Science and Pollution Research*. https://doi.org/10.1007/s11356-016-7109-z

Vilmin, L., Flipo, N., Escoffier, N., Rocher, V., & Groleau, A. (2016). Carbon fate in a large temperate human-impacted river system: Focus on benthic dynamics. *Global Biogeochemical Cycles*, *30*, 1086–1104. https://doi.org/10.1002/2015GB005271

Waliser, D., & Guan, B. (2017). Extreme winds and precipitation during landfall of atmospheric rivers. *Nature Geoscience*, *10*(3), 179–183. https://doi.org/10.1038/ngeo2894

Wyatt, K. H., Turetsky, M. R., Rober, A. R., Giroldo, D., Kane, E. S., & Stevenson, R. J. (2012). Contributions of algae to GPP and DOC production in an Alaskan fen: Effects of historical water table manipulations on ecosystem responses to a natural flood. *Oecologia*, *169*(3), 821–832. https://doi.org/10.1007/s00442-011-2233-4

Yarwood, R. R., Rockhold, M. L., Niemet, M. R., Selker, J. S., & Bottomley, P. J. (2006). Impact of microbial growth on water flow and solute transport in unsaturated porous media. *Water Resources Research*, *42*, W10405. https://doi.org/10.1029/2005WR004550

Zarnetske, J. P., Haggerty, R., Wondzell, S. M., & Baker, M. A. (2011). Labile dissolved organic carbon supply limits hyporheic denitrification. *Journal of Geophysical Research*, *116*, G04036. https://doi.org/10.1029/2011JG001730

Zarnetske, J. P., Haggerty, R., Wondzell, S. M., Bokil, V. A., & González-Pinzón, R. (2012). Coupled transport and reaction kinetics control the nitrate source-sink function of hyporheic zones. *Water Resources Research*, *48*, W11508. https://doi.org/10.1029/2012WR011894

Zhang, Y., Hubbard, S., & Finsterle, S. (2011). Factors governing sustainable groundwater pumping near a river. *Ground Water*, *49*(3), 432–444. https://doi.org/10.1111/j.1745-6584.2010.00743.x

Zhou, Y., Ritzi, R. W., Soltanian, M. R., & Dominic, D. F. (2014). The influence of streambed heterogeneity on hyporheic flow in gravelly rivers. *Groundwater*, *52*(2), 206–216. https://doi.org/10.1111/gwat.12048